ELSEVIER

Early diagenesis of trace metals (Cd, Cu, Co, Ni, U, Mo, and V) in the freshwater reaches of a macrotidal estuary

Stéphane Audry *, Gérard Blanc, Jörg Schäfer, Gwénaëlle Chaillou [1], Sébastien Robert

"Traceurs Géochimiques et Minéralogiques (T.G.M.)" team, UMR CNRS 5805 EPOC, Université Bordeaux 1, Avenue des facultés, 33405 Talence cedex, France

Abstract

Vertical profiles from the water column, including the maximum turbidity zone (MTZ) to the consolidated sediment were sampled in September 2000 in the freshwater reaches of the Gironde Estuary during a complete neap tide-spring tide cycle. The vertical distributions of dissolved major redox parameters and metals (Mn, Fe, Cd, Cu, V, Co, Ni, Mo, and U) were determined. Reactive particulate metal fractions were also determined from selective leaching. The studied system is characterized by density layers functioning at different time-scales, consisting of two mobile layers, i.e., the liquid (LM) and the soft mud (SM), overlying consolidated sediments (CS). This results in a three-zone diagenetic regime where (1) O_2 dynamics are fast enough to show depletion in the rapidly mixed LM sequence (tidal time-scale), (2) denitrification occurs on the weekly time-scale mixing SM sequence, and (3) the Mn, Fe, and sulfate cycling occurs in the CS layer (annual time-scale). The studied trace metals show differential behavior during early diagenesis: (1) Cd, Cu, and V are released into pore water preferentially from organic matter in the SM, (2) Co, Ni, and U are released in the CS from Mn and Fe oxides during reductive dissolution, and (3) Mo from both processes. Transient conditions (i.e., oscillations of redox fronts and reoxidation processes), due to the dynamics of the mobile layers, strongly influence the trace metal distributions as inducing resolubilization (Cd, Cu, and Mo). In the CS, authigenic metal phases accumulate, either by direct precipitation with sulfides (Cu, Cd) or co-precipitation with Fe-sulfides (Mo). Microbially mediated reduction of Fe oxides is proposed to control U removal from pore water by reduction of U(VI) to U(IV) at depth. However, a significant fraction of the trace metals is trapped in the sediment in exchangeable forms, and therefore is susceptible to be mobilized due to resuspension of estuarine sediment during strong river flood periods and/or dredging activities.
© 2006 Elsevier Inc. All rights reserved.

1. Introduction

Estuaries play an important role in the transfer of pollutants, including trace metals, from continent to ocean. They are mixing-zones between marine, coastal and fluvial waters, and therefore are considered as reactive zones for fluvial inputs (Shink, 1981). Mixing of waters characterized by different physical, chemical, and biological properties induces changes in trace metal partitioning between particulate and dissolved phases (e.g., Turner and Millward, 1993; Elbaz-Poulichet et al., 1996; Guieu et al., 1998). This redistribution is a key issue as it determines the mobility and the toxicity of trace metals within estuaries and coastal oceans. Trace metal transformations have been extensively studied in numerous estuaries (e.g., Morris et al., 1982; Lasslet and Balls, 1995; Kraepiel et al., 1997; Tang et al., 2002) and have been mainly explained by flocculation, chloride complexation by salinity effect and oxidation–reduction processes in the surface sediment (Chiffoleau et al., 1994; Zwolsman et al., 1997). Moreover, it has been shown that in macrotidal estuaries, the presence of a maximum turbidity zone (MTZ) can strongly influence trace metal mobilization by occurrence of oxidation–reduction processes in the water column similar to those taking place

---

* Corresponding author.

E-mail addresses: s.audry@epoc.u-bordeaux1.fr (S. Audry), g.blanc@epoc.u-bordeaux1.fr (G. Blanc).

[1] Present address: Earth and Planetary Sciences, McGill University, Montreal, Que., Canada H3A 2A7.

in surface sediment (Abril et al., 2000; Robert et al., 2004). Nevertheless, oxidation–reduction processes within the MTZ are still poorly understood and, most of the time, their contribution to the release of dissolved trace metals in the system is not taken into account.

The aim of this study is to assess the oxidation–reduction processes occurring during early diagenesis and their impact on the redistribution of Fe, Mn, and trace metals (Cd, Co, Ni, Cu, Mo, U, and V) in the macrotidal Gironde Estuary, which is strongly impacted by trace metal pollution. High-resolution ($\sim$cm) vertical profiles of dissolved, total and reactive particulate metal concentrations are combined with major redox parameters, measured from the water column (WC) to the consolidated sediment (CS) during four contrasted tidal situations. In order to avoid interference by salinity-induced processes (e.g., chloride complexation) that could mask diagenetic processes, sampling was performed in the upstream freshwater reaches of the estuary. Accordingly, this work aims to characterize estuarine redox processes in the WC–CS system as a reference for understanding trace metal behavior in the downstream estuary where additional geochemical gradients occur, as well as for other highly turbid estuaries. Furthermore, based on these results, we propose a conceptual model of transient behavior of selected metals during early diagenesis for highly turbid estuaries.

2. Background and methods

2.1. The gironde estuary

The Gironde estuary is known for its polymetallic pollution resulting from mining and smelting activities since the late 19th century (e.g., Latouche, 1988; Grousset et al., 1999; Blanc et al., 1999; Schäfer et al., 2002; Audry et al., 2004). The main point source of trace metals was identified in the upper part of the Lot River, a tributary of the Garonne River (Boutier, 1981; Latouche, 1992), where a small stream (the Riou-Mort River) drains a waste pit area of a now-abandoned zinc-ore manufacturing facility.

The Gironde Estuary (Fig. 1) is a partially mixed to well-mixed macrotidal estuary with tidal amplitude from 1.5 to 5.5 m. During the tidal cycle, ocean water inputs are 30–40 times higher than fluvial inputs (Allen et al., 1977). The mean annual fluvial water input calculated over the 1990–1999 period was about 34×10^9 m^3 a^{-1} (Schäfer et al., 2002). The residence time of fluvial water in the estuary is estimated to be 20 and 86 days during high and low water discharge periods, respectively, and that of particles approximately 2 a (Jouanneau and Latouche, 1981). For navigation purposes, the estuary is continuously dredged. Typically, an average of about 8.85×10^6 t of particles are dredged annually, corresponding to a mean daily sediment mass of 24,000 t. Asymmetrical progression of the tidal wave toward the upstream estuary results in the presence of a MTZ with suspended particulate matter (SPM) concentrations in surface water higher than 1 g L^{-1} (Castaing,

1981). The MTZ is often located in the low salinity zone but can move up and down the estuary depending on seasonal river flow variations (Sottolichio and Castaing, 1999). Sediment resuspension generally occurs during erosion periods at mid-ebb and mid-flood while tidal slacks are sedimentation periods. The model of the density layers of the Gironde Estuary was previously described in detail by Robert et al. (2004) and is presented in Fig. 2.

2.2. Sample collection and handling

In September 2000, sampling of the MTZ–SM–CS continuum (see Fig. 2) was conducted aboard a river boat in the freshwater reaches ($S < 0.1$) of the Gironde Estuary (KP-3; Fig. 1) at low fluvial discharge (440 m^3 s^{-1}). During this period, neap (6th–9th of September) and spring (14th–17th of September) tide situations were sampled at the same sampling point during both high and low tide slacks, resulting in four vertical profiles. Sampling was done using two samplers specifically designed to simultaneously collect samples from the MTZ–SM–CS continuum (Robert et al., 2004). The first sampler is a box-sampler enabling retrieval of WC samples with a 20 cm-resolution and was described in detail by Abril et al. (2000). The second sampler is a 2.6-m interface corer consisting of a 10×10-cm rectangular Plexiglas tube. This device permits sampling of the uppermost decimeters of the CS, the undisturbed SM–CS boundary and the overlying WC. Collection of samples was done with a 5-cm sampling resolution from the WC to the CS and with a resolution of up to 0.5 cm in the CS. Cores of the CS were sliced in thin horizontal sections with a plastic cutter. All samples were immediately collected in acid-cleaned 200 mL propylene centrifuge vials and centrifuged at 5000 rpm for 15 min under a N$_2$ atmosphere. For each sample, the supernatant was filtered through cellulose acetate syringe filters (0.2 μm porosity; Sartorius®) and then divided into three aliquots for nutrient, sulfate and chloride, and metal analyses. Aliquots for nutrient analysis were stored in 5-mL polycarbonate tubes and immediately frozen at -20 °C until analysis; aliquots for sulfate and chloride analysis were stored in 14-mL polypropylene tubes and kept at 4 °C; aliquots for trace metal measurements were stored in acid-cleaned tubes, acidified (pH $\sim$ 1; HNO$_3$ ultrapure 1‰) and stored at 4 °C.

2.3. Pore water analysis

Dissolved O$_2$ and pH measurements were done with an ISY™52 oximeter and a calibrated WTW profilLine 197 pH-meter with SenTix 21 electrode, respectively, on non-centrifugated aliquots. Sulfate and chloride concentrations were analyzed by ion chromatography (Dionex DX-120 chromatograph) using the AFNOR (1996) method. The detection limit for sulfate and chloride was 2 mg L^{-1}. Accuracy was better than 5% and reproducibility better than 3%. Salinity was then deduced from the chloride
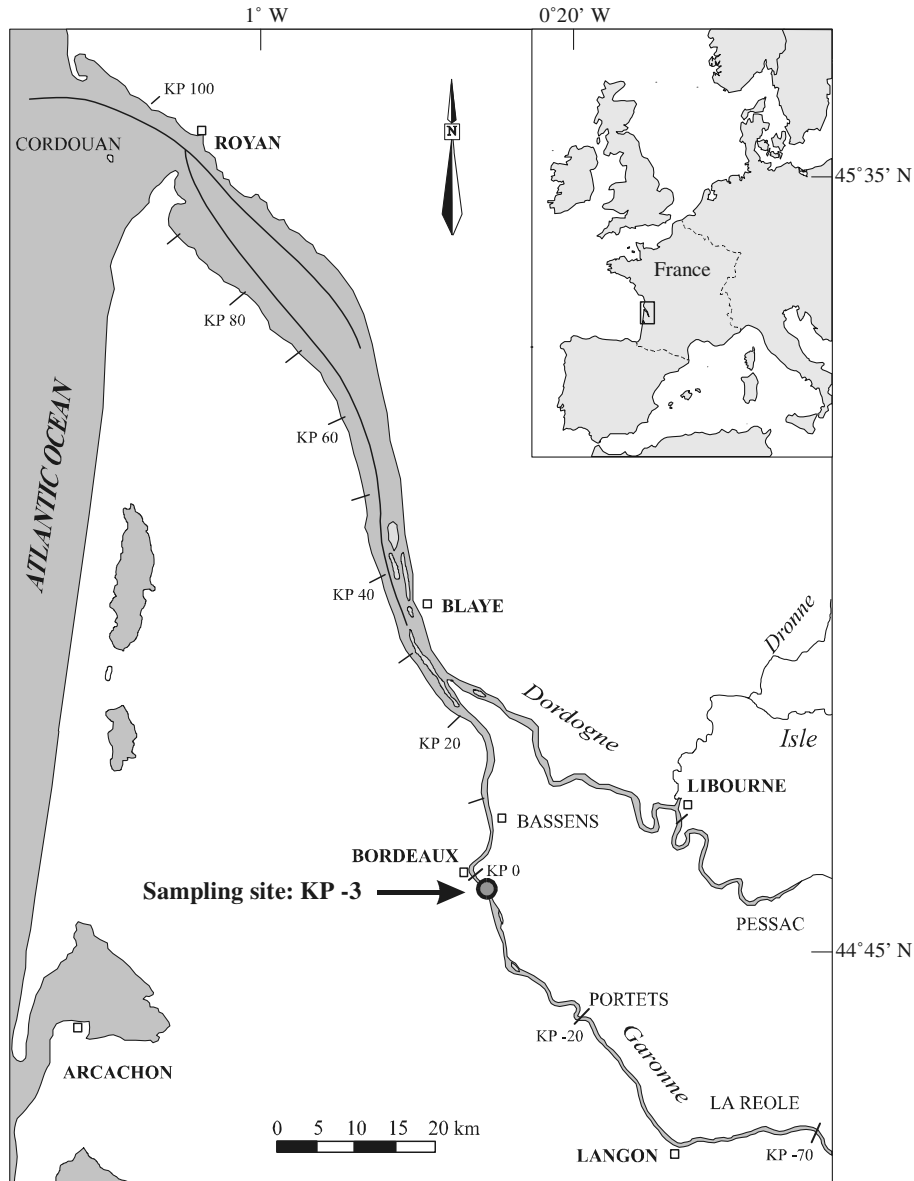
Fig. 1. Map of the Gironde Estuary showing the sampling site. KP as the distance (in km) from the city of Bordeaux.
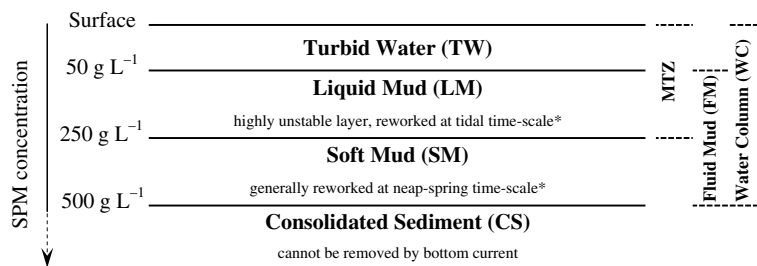

Fig. 2. Schematic representation of the density layers in the Gironde Estuary water column. MTZ: maximum turbidity zone; SPM: suspended particulate matter. *Abril et al. (1999).

concentrations. Nitrate was measured by flow injection analysis (FIA) according to Anderson (1979). Ammonia was analyzed with the FIA method described by Hall and Aller (1992). Total dissolved Fe concentrations were measured with the colorimetric method using ferrozine (Stookey, 1970; Viollier et al., 2000). Dissolved Mn^{2+} was determined by double-beam FAAS (Perkin-Elmer 420). For both Fe and Mn, accuracy and reproducibility were better than 5%. The detection limits for Fe and Mn were $<1\,\mu M$ and $<200\,nM$, respectively.

2.4. Solid analysis

Determination of SPM concentrations was performed by filtration through dry pre-weighted filters (Whatman GF/F, 0.7 μm). The filters were dried to constant weight (45 °C) and then re-weighed. Grain size measurements were performed with a laser granulometer (Malvern Mastersizer). Particulate organic carbon (POC) was measured from the dry, powdered and homogenized material using a carbon/sulfur analyzer (LECO, CS-125) according to Cauwet et al. (1990). Inorganic carbon (i.e., carbonate) was eliminated by HCl addition prior to analysis.

Single chemical extractions (i.e., using a separate aliquot of the same sample for each reagent) were applied on the neap tide-high tide samples. The single extraction procedures used in this study are principally based on the sequential extraction scheme according to Tessier et al. (1979). Tack et al. (1996) and Alborés et al. (2000) showed that similar results for trace metal partitioning (Cu, Cr, Ni, Pb, and Zn) were obtained from the conventional Tessier et al. (1979) sequential extraction method and from single extractions using identical operating conditions applied in each individual extraction. Single extractions were chosen over sequential extractions in order to avoid some limitations of the latter. These limitations are (1) possible changes in elemental speciation during the successive extraction steps, (2) changes or losses of elemental species during the residue washing step (Rosenberg and Ariese, 2001)

and (3) multiple risks of sample contamination from the successive reagents used (Quevauviller, 1998). The single extraction protocols and the four operationally defined target fractions are presented in Table 1.

2.5. Trace metal measurements

Dissolved and particulate trace metal concentrations were measured using ICP-MS (Elan 5000, Perkin-Elmer). The analytical methods employed were quality checked by analysis of certified international reference water (SLRS-4; Table 2). Total sediment digestion included method blanks and digestion of certified international reference material (PACS-1; Table 2). Accuracy was within 5% of the certified values and the analytical error (rsd) generally better than 5% for concentrations 10 times higher than the detection limits.

3. Results and discussion

3.1. Water column-consolidated sediment boundary

In the concentration–depth profiles, depth is reported using the distance from the SM–CS boundary. The high resolution of the salinity profiles (Figs. 3a and b) permits distinguishing the four contrasted tidal situations, even for salinity lower than 0.1. In the WC, salinity is higher at high tide compared to low tide, and this difference is

Table 1
Operating conditions applied for the single extraction procedures

Fraction	Sample weight (mg)	Reagent	Shaking time, temperature	Reference
Exchangeable/ carbonate	500	10 mL NaOAc 1 M + HO Ac (pH 5)	5 h at 25 °C	Tessier et al. (1979)
		ph adjustment with HOAc 5 M during the extraction		
Fe/Mn oxides (reducible)	200	12.5 mL ascorbate solution (pH = 8)	24 h at 25 °C	Kostka and Luther (1994)
Organic matter/ sulfides (oxidizable)	1000	8 ml H_2O_2 30% m/v + NaOH (pH = 5)	2 h at 85 °C	Tessier et al. (1979) modified
		then 3 mL H_2O_2 30% m/v + NaOH	2 h at 85 °C	Ma and Uren (1995)
		then 5 mL NH_4OAc 1 M + 20 mL H_2O milli-Q	30 min at 25 °C	
Total metal content	30	HCl 12 N + HNO_3 14 N + HF 26 N	2 h at 110 °C	Schäfer et al. (2002)

Table 2
Results obtained (mean ± standard deviation) from ICP-MS analysis of certified reference materials

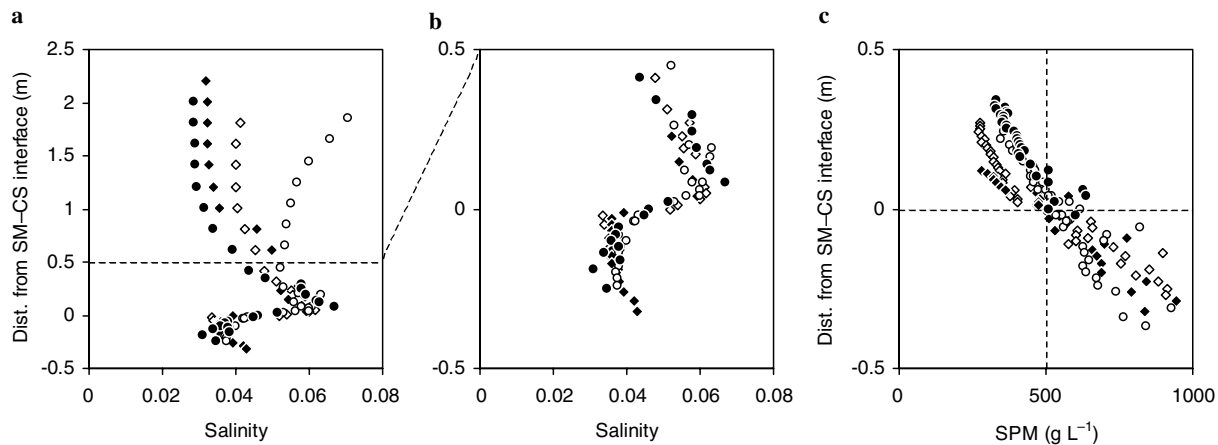|	SLRS-4 ($n = 20$)		PACS-1 ($n = 10$)	
	Certified value (μg L^{-1})	Measured value (μg L^{-1})	Certified value (mg kg^{-1})	Measured value (mg kg^{-1})
Cd	0.012 ± 0.002	0.012 ± 0.003	2.38 ± 0.20	2.55 ± 0.15
Cu	1.81 ± 0.08	1.84 ± 0.09	452 ± 16	449 ± 17
Ni	0.67 ± 0.08	0.69 ± 0.09	44.1 ± 2.0	42.2 ± 1.7
Co	0.033 ± 0.006	0.032 ± 0.005	17.5 ± 1.1	18.3 ± 0.9
Mo	0.21 ± 0.02	0.22 ± 0.03	12.9 ± 0.9	13.0 ± 0.7
U	0.050 ± 0.003	0.049 ± 0.003	—	—
V	0.32 ± 0.03	0.34 ± 0.04	127 ± 5	131 ± 6

Fig. 3. Depth profiles for salinity (a and b) and SPM concentrations (c) at neap tide-low tide (◆), neap tide-high tide (◇), spring tide-low tide (●), and spring tide-high tide (○).

more contrasted at spring tide than neap tide. In contrast, the lower part of the cores is characterized by similar profiles, showing an inversion in salinity (Fig. 3b). The salinity–inversion layer defines the SM–CS boundary and shows SPM concentration of ~500 g L^{-1} (Fig. 3c). This result is in agreement with hydrodynamic studies that define sediments with particle concentrations greater than 500 g L^{-1} as consolidated (Bassoulet and Le Hir, 1997; Sottolichio and Castaing, 1999). The consistent similarity of the salinity profiles in the SM layer suggests that the SM bottom is preserved between the neap tide and the spring tide situations and that only the upper part of the SM is resuspended. The four sampled situations show different SM thickness, from 15 to 30 cm (see Figs. 6–9).

3.2. Total particulate metals

Total particulate Fe and Mn show more or less constant values above and below the SM–CS boundary, centered on 41,100 µg g^{-1} for Fe and 1050 µg g^{-1} for Mn (Fig. 4a). The SM–CS boundary is characterized by the decrease of total Fe and Mn concentrations, down to 22,250 and 689 µg g^{-1}, respectively. Such decrease is likely related (at least partly) to a sandy layer present at the SM–CS boundary shown by the bimodal grain size distribution (up to 5% > 100 µm; Fig. 4b). In contrast, the upper and lower parts of the core are characterized by unimodal grain size distribution showing finer grain size (Figs. 4a and c).

Total particulate trace metal concentration–depth profiles are similar to that of Fe and Mn, with more or less constant concentrations above and below the SM–CS boundary (i.e., ~125, 55, 30, 18, and 3 µg g^{-1} for V, Ni, Cu, Co, and U, respectively) and lower concentrations due to grain size effect at the SM–CS boundary (Figs. 4c–g). Cadmium and Mo profiles show higher variability with total concentrations ranging from 0.6 to 1.5 µg g^{-1} and from 0.4 to 1.4 µg g^{-1}, respectively (Figs. 4b and h).

3.3. Sediment redox conditions

This distribution of major dissolved redox species is characterized by concentration gradients driven by the bacterially mediated oxidation of organic matter (OM) (Froelich et al., 1979; Postma and Jakobsen, 1996). The distribution globally shows the same pattern for the four tidal situations (Figs. 6–9).

3.3.1. Oxygen and pH
Dissolved oxygen and pH measurements were only performed on the less turbid samples (i.e., above the LM–SM boundary), as these measurements require a minimum volume of water that could not be extracted from the most turbid samples. For the different sampled situations, pH values in the WC range from 7.7 to 8.5 but are relatively constant (variability <0.5) within each tidal situation (see electronic annex EA-1). The LM is partially oxygen-depleted, showing strongly decreasing O$_2$ concentrations from ~180–200 µM in the upper part of this layer to 25–65 µM above the LM–SM boundary (Fig. 5). This indicates that oxic mineralization of OM proceeds in this layer and highlights the high oxidant demand of the Gironde Estuary freshwater sediments. Although measurements of dissolved O$_2$ in the SM are not available, the SM is assumed to be anoxic, indicated by nitrate consumption in this layer (as discussed below; Figs. 6a–9a) and in agreement with data reported by Robert et al. (2004) for the same estuary.

3.3.2. Nitrate
Nitrate concentrations above the LM–SM boundary range from 95 to 140 µM (Figs. 6a–9a) and stay relatively constant in the upper WC. Nitrate then rapidly decreases in the SM to concentration below the detection limit due to bacterial denitrification in this layer. In our system, where the LM is typically reworked at tidal time-scale (Abril et al., 1999; Fig. 2), the near-linear NO$_3^-$ concentration gradient across the LM–SM boundary for all four tidal situations reflects diffusive exchange between sink (SM
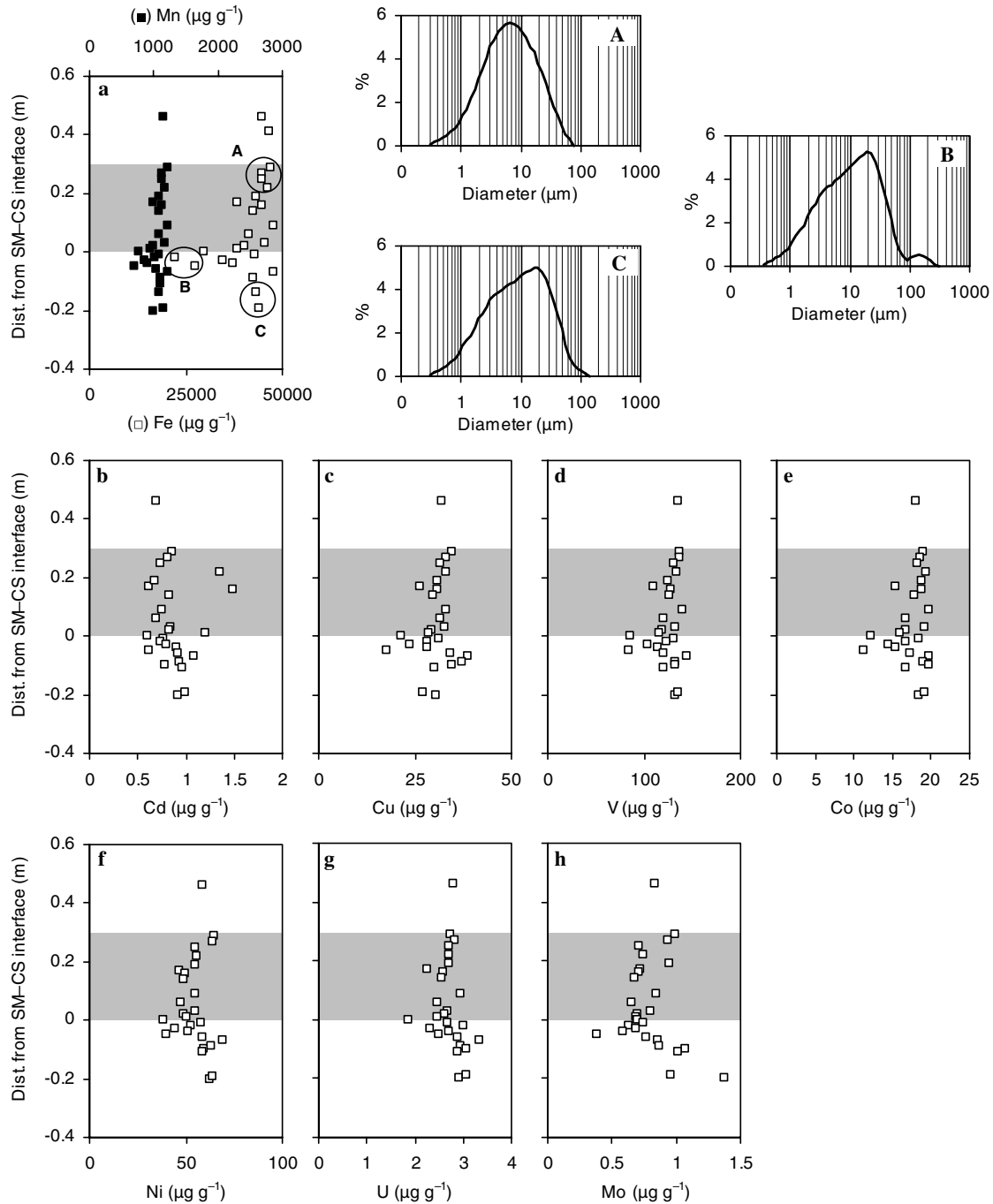
Fig. 4. Concentration–depth profiles for particulate Fe, Mn (a) and trace metal (b–h) as determined from total digestion from the core for the neap tide-high tide situation. Also shown, the grain size distributions representative of the upper soft mud (A), the soft mud–consolidated sediment boundary (B), and the bottom core consolidated sediment (C). Grey area represents the soft mud layer.

layer) and source (LM layer) of NO_3^- while the upper boundary of the NO_3^- gradient indicates a physical boundary created by the time-dependent mixing events. Therefore, the top of the gradients may be interpreted as the transition between an advective (LM layer) and a diffusive (SM layer) system. The LM resuspension exerts a strong physical control on the microbial community present in this layer. At the time-scale of LM settling and persistence (i.e., few hours), oxic mineralization of OM does not proceed fast enough to consume the initial O_2 pool (180–200 µM; Fig. 5) before resuspension, thus not allowing the facultative anaerobes presumably present in the LM (Abril et al., 2000) to perform denitrification. By favoring the mixing of suboxic pore water with more oxygenated water and the regeneration of the reactive organic material pool, resuspension favors oxic respiration and high OM mineralization in the LM during the tidal slack. Denitrification in the SM is also influenced by the vertical dynamics of the LM particles. During tidal slacks, NO_3^- concentration in the LM bottom tends to decrease due to diffusion
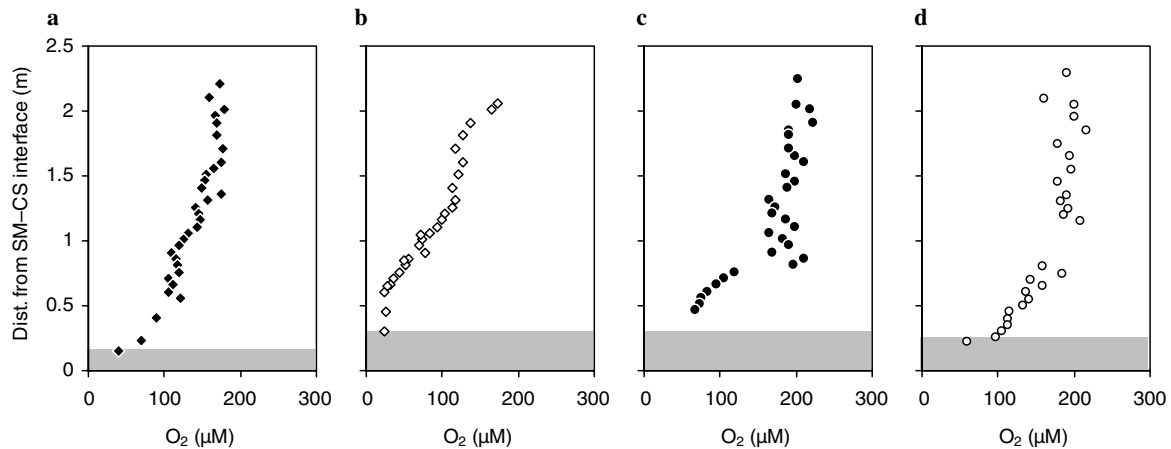
Fig. 5. Dissolved O_2 concentration–depth profiles for neap tide-low tide (a), neap tide-high tide (b), spring tide-low tide (c) and spring tide-high tide (d). Grey area represents the soft mud layer.

towards the denitrification zone located in the SM. If there was no LM resuspension, the NO_3^- concentration gradient would decrease with time, resulting in probably lower rate of denitrification. By providing nitrate-rich pore water at each tidal slack, the LM cycle of settling-resuspension maintains high downward NO_3^- diffusion and thus likely controls the denitrification rate in the SM. Assuming that the SM is partially reworked at neap tide-spring tide time-scale, the freshly deposited SM initially should contain nitrate-rich pore water. However, at spring tide-high tide the SM is totally nitrate-depleted (Fig. 9a), suggesting a weekly time-scale for NO_3^- consumption in the SM.

3.3.3. Sulfate and sulfide

Dissolved SO_4^{2-} shows constant concentrations in the WC (0.25–0.28 mM; Figs. 6c–9c) and then sharply decreases below the SM–CS boundary to rapidly reach levels lower than the detection limit, which is attributed to sulfate reduction in the CS. However, within this zone, small peaks of SO_4^{2-} (~0.05 mM) are observed for spring tide (Figs. 8c and 9c). The interpretation of the SO_4^{2-} consumption in terms of SO_4^{2-} reduction in the CS is supported by the associated NH_4^+ production in this layer (Figs. 6b–9b). Interestingly, slight SO_4^{2-} enrichments (0.02–0.07 mM) are observed close to the SM–CS boundary for all four tidal situations (Figs. 6c–9c). The excess SO_4^{2-} can be attributed to oxidation of dissolved sulfide diffusing from the sulfate-reduction zone (i.e., CS zone). Oxygen, that could possibly be present within micro-environments in the anoxic SM, is not considered a potential oxidant as the reaction of dissolved sulfides with O_2 is not thermodynamically favorable (Luther and Ferdelman, 1993). Bacterial production of sulfate from reduced sulfur coupled to NO_3^- reduction (Suits and Arthur, 2000) is unlikely here, as the observed excess SO_4^{2-} occurs at depth were the SM is nitrate-depleted. Therefore, the SO_4^{2-} production is assigned to anaerobic oxidation of upward diffusing sulfides by Mn and/or Fe oxides (Aller and Rude, 1988; Canfield, 1989;

Burdige, 1993; Yao and Millero, 1996; Böttcher and Thamdrup, 2001; Shippers and Jørgensen, 2001).

While dissolved sulfides were not analyzed, their potential concentration in the CS can be roughly estimated from SO_4^{2-} concentrations. From the SO_4^{2-} concentrations observed above the LM–SM boundary (Figs. 6c–9c), we estimate that complete pore water SO_4^{2-} reduction may produce a dissolved sulfide concentration of ~3 mM. This potentially available dissolved sulfide concentration may be limited by oxidation due to upward diffusion and oscillations of redox fronts. However, the greatest SO_4^{2-} peak observed (up to 0.33 mM in the spring tide-high tide core; Fig. 9c) suggests that the amount of sulfide consumed by oxidation should represent less than 20% of the reactive (amorphous or dissolved) sulfide present at the respective depth.

3.3.4. Manganese

Dissolved Mn becomes detectable just above the SM–CS boundary for low tide and immediately increases sharply (Figs. 6e and 7e). In contrast, for high tide, dissolved Mn is detected at the LM–SM boundary or just below and remains more or less constant in the SM (4–6.5 μM) before increasing drastically at a similar depth to that for low tide (Figs. 8e and 9e). The production of dissolved Mn is ascribed to reductive dissolution of Mn oxides, which is supported by the concomitant decrease of Mn extracted by the ascorbate leaching (Mn_{asc}) from ~350 μg g^{-1} 3 cm above the SM–CS boundary to 68 μg g^{-1} in the CS (Fig. 10a) and in agreement with results from previous studies on the Gironde Estuary (e.g., Tseng et al., 2001; Robert et al., 2004). The pool of Mn_{asc} data in the CS characterized by higher concentrations (215–340 μg g^{-1}; Fig. 10a) is attributed to less-reactive Mn oxides that do not readily undergo reductive dissolution. Increasing Mn concentrations in sediment pore water occur only when overlying bottom waters are oxygenated, thus permitting Mn oxide precipitation from upward diffusing dissolved Mn in the surface sediment (Calvert and Pedersen, 1993). Therefore,
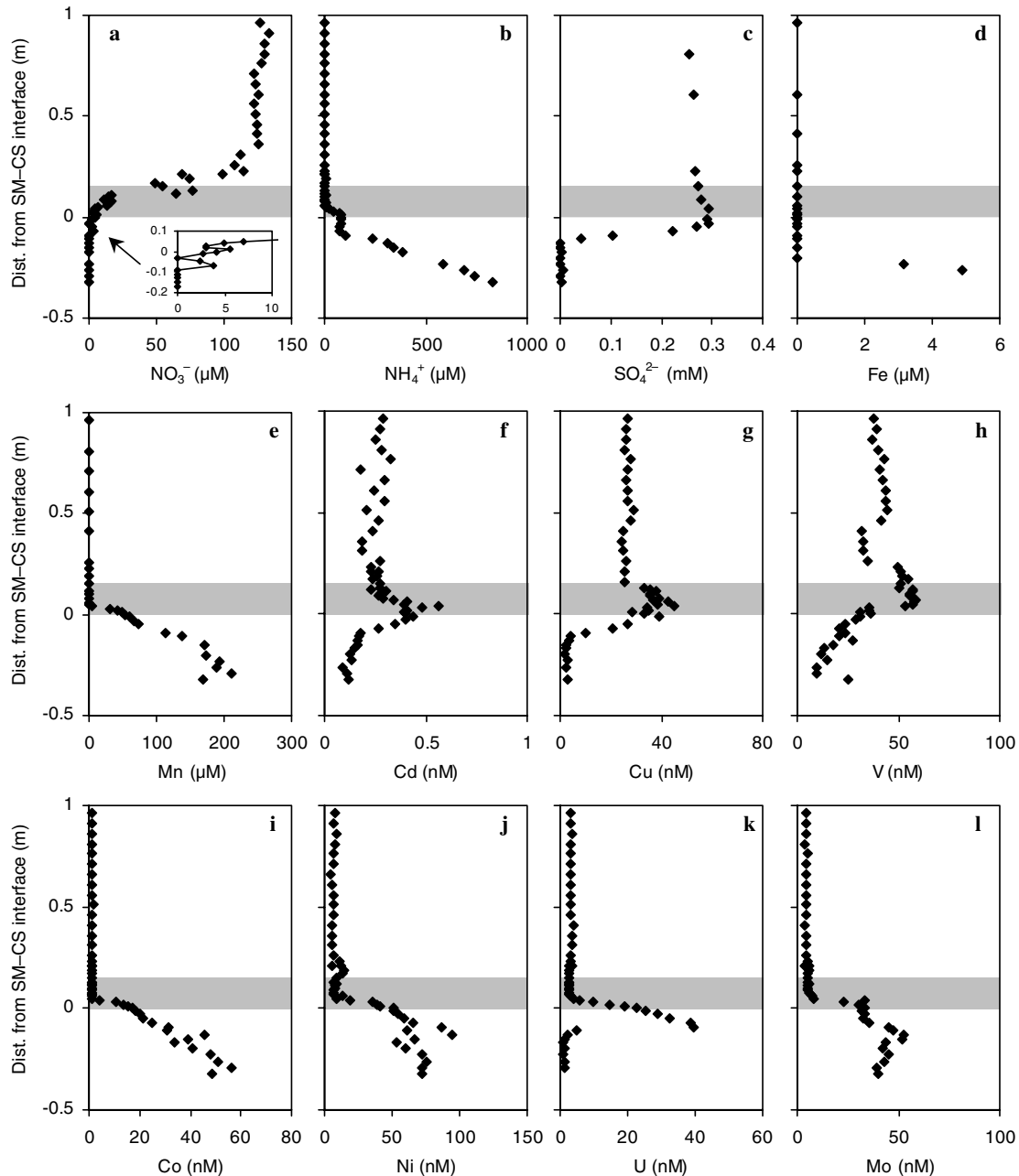
Fig. 6. Concentration–depth profiles for N-species (a and b), sulfate (c), Fe and Mn (d and e) and trace metals (f–l) at neap tide-low tide. The soft mud layer (grey area) is 15-cm thick.

the strong dissolved Mn gradients observed in the CS suggest that oxic conditions in the WC prevail most of the year and that the presence of an anoxic SM over the CS is restricted to low water periods. Hence, this result suggests an annual time-scale for the Mn cycling in the CS of the Gironde Estuary.

At the bottom of the cores, dissolved Mn concentrations reach concentrations of about 200–250 μM and then show slight decreases for neap tide and spring tide-low tide (Figs. 6e–8e). These decreases may be attributed to Mn carbonate precipitation (e.g., Whiteley and Pearce, 2003), which is supported by the increase of particulate

Mn extracted by NaOAc (Mn_{NaOAc}) from 260 to 600 μg g^{-1} from the SM–CS boundary (Fig. 10i) and the positive relationship between Mn_{NaOAc} and inorganic carbon (not shown). However, Mn precipitation with carbonate at the SM–CS boundary is not compatible with the pore water profile that suggests removal of dissolved Mn only 10 cm below the SM–CS boundary (Fig. 7e). Manganese from other solid phases than carbonate, as oxides (Martin et al., 1987) and OM (Slaveck et al., 1982) can be extracted by the NaOAc leaching. This lack of selectivity may explain the discrepancy between the dissolved Mn and Mn_{NaOAc} profiles.
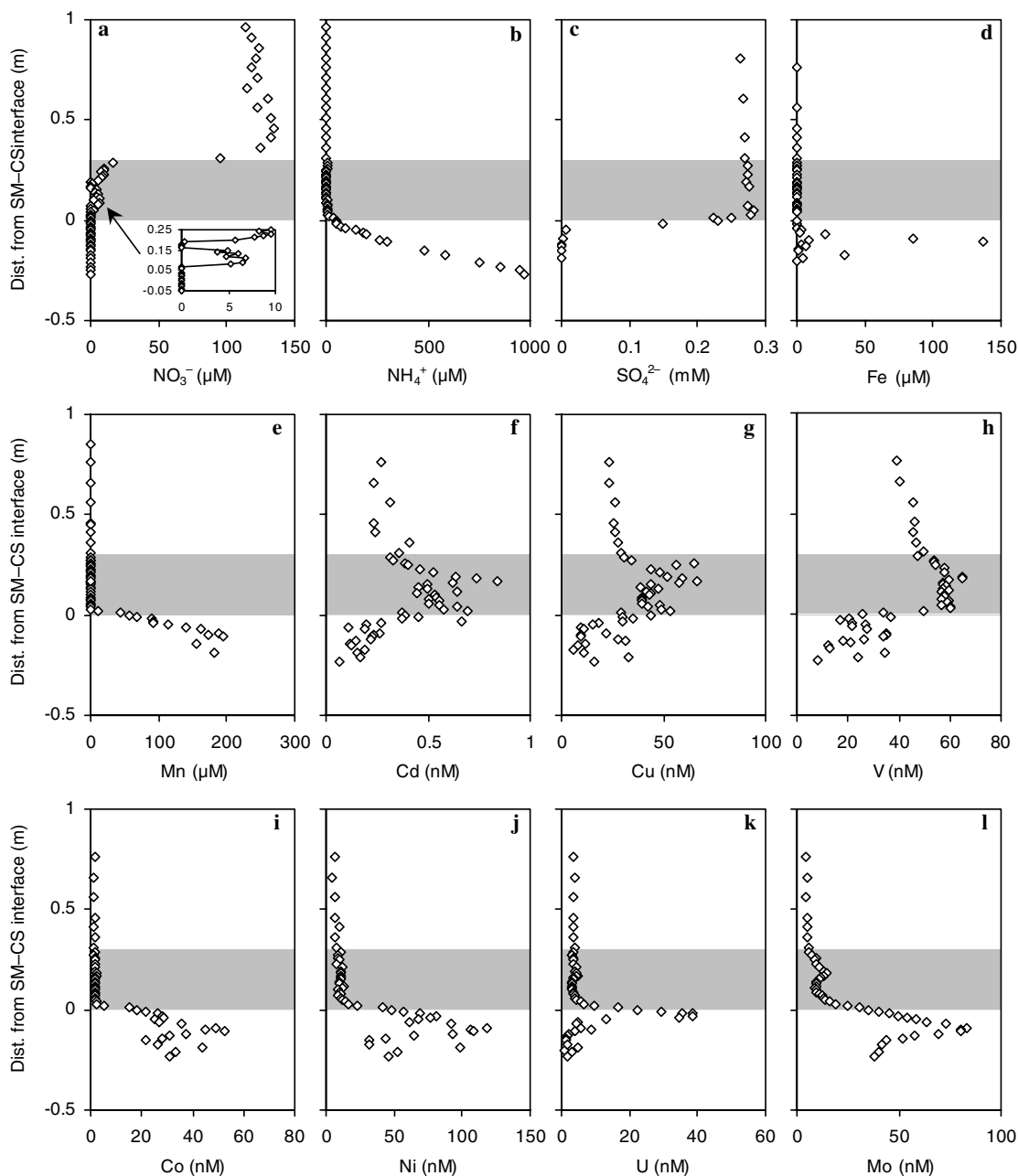
Fig. 7. Concentration–depth profiles for N-species (a and b), sulfate (c), Fe and Mn (d and e) and trace metals (f–l) at neap tide-high tide. The soft mud layer (grey area) is 30-cm thick.

3.3.5. Iron

Dissolved Fe shows strong and increasing concentration gradients in the CS for neap tide-low tide and spring tide-high tide while, in contrast, dissolved Fe reaches maximum concentrations of 150 μM for neap tide-high tide and 20 μM for spring tide-low tide (Figs. 6d–9d). The production of dissolved Fe in the CS reflects the reduction of Fe oxides partly by reaction with dissolved sulfides (Poulton, 2003) likely present in the sediment at these depths and microbially mediated reaction (e.g., Rosenthal et al., 1995). The reduction of Fe oxides in the CS is supported by the production of NH_4^+ in this layer (Figs. 6b–9b).

Reductive dissolution of Fe oxides and sulfate reduction appear to occur at the same depth at the sampling resolution (Figs. 6–9c and d). The overlap of redox boundaries, while not in line with the typical redox depth-sequence established by Froelich et al. (1979) which predicts reductive dissolution of Fe oxides prior to sulfate reduction and which is now considered as an oversimplification (e.g., Canfield, 1993), has been previously reported in estuarine (Widerlund and Ingri, 1995) and sulfidic marine (Boesen and Postma, 1988) environments. The ascorbate leaching is designated to extract the most reactive Fe oxide fraction (amorphous oxides) (Kostka and Luther, 1994; Anschutz et al., 1998).
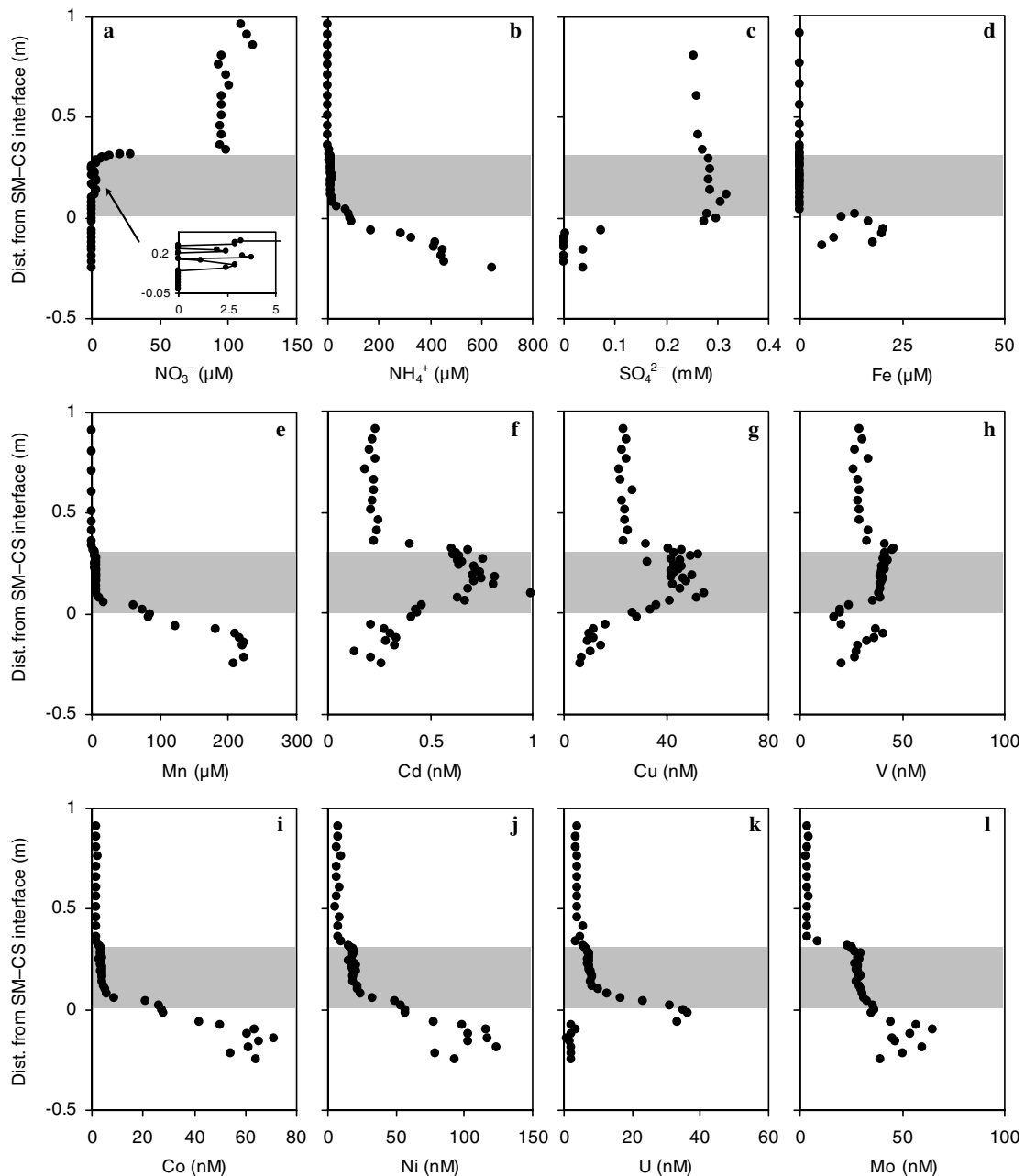
Fig. 8. Concentration–depth profiles for N-species (a, b), sulfate (c), Fe and Mn (d and e) and trace metals (f–l) at spring tide-low tide. The soft mud layer (grey area) is 30-cm thick.

Iron extracted by ascorbate is very low (2–6% of the total Fe content; see electronic annex EA-2), suggesting that about 95% of the Fe oxides present in the Gironde Estuary sediments have a stability close to goethite and hematite. Under these conditions, and given the similarities of the total free energy for sulfate reduction and reduction of Fe oxides at circumneutral pH (Stumm and Morgan, 1996), simultaneous equilibrium between sulfate reduction, reduction of Fe oxide and FeS is expected (Postma and Jakobsen, 1996) in the sulfidic CS of the Gironde Estuary. Dissolved Fe decreases (spring tide-low tide; Fig. 8d) or is totally re-moved from pore water (neap tide-high tide; Fig. 7d) in

the CS due to FeS precipitation. Using the mean Fe concentration extracted by the ascorbate leaching (90 mg kg^{-1}; see electronic annex EA-2), we estimate that about 0.8 mM of dissolved Fe might be potentially released in the CS due to reductive dissolution of reactive Fe oxides. This value is of the same order of magnitude as that of dissolved sulfides potentially present in the CS. Given the typically fast reaction (milliseconds or less) of dissolved Fe with dissolved sulfides (Rickard, 1995; Chadwell et al., 1999, 2000), the pore water concentration of Fe, and therefore its mobility, could be easily controlled by sulfides through Fe-sulfide precipitation in the sulfidic zone.
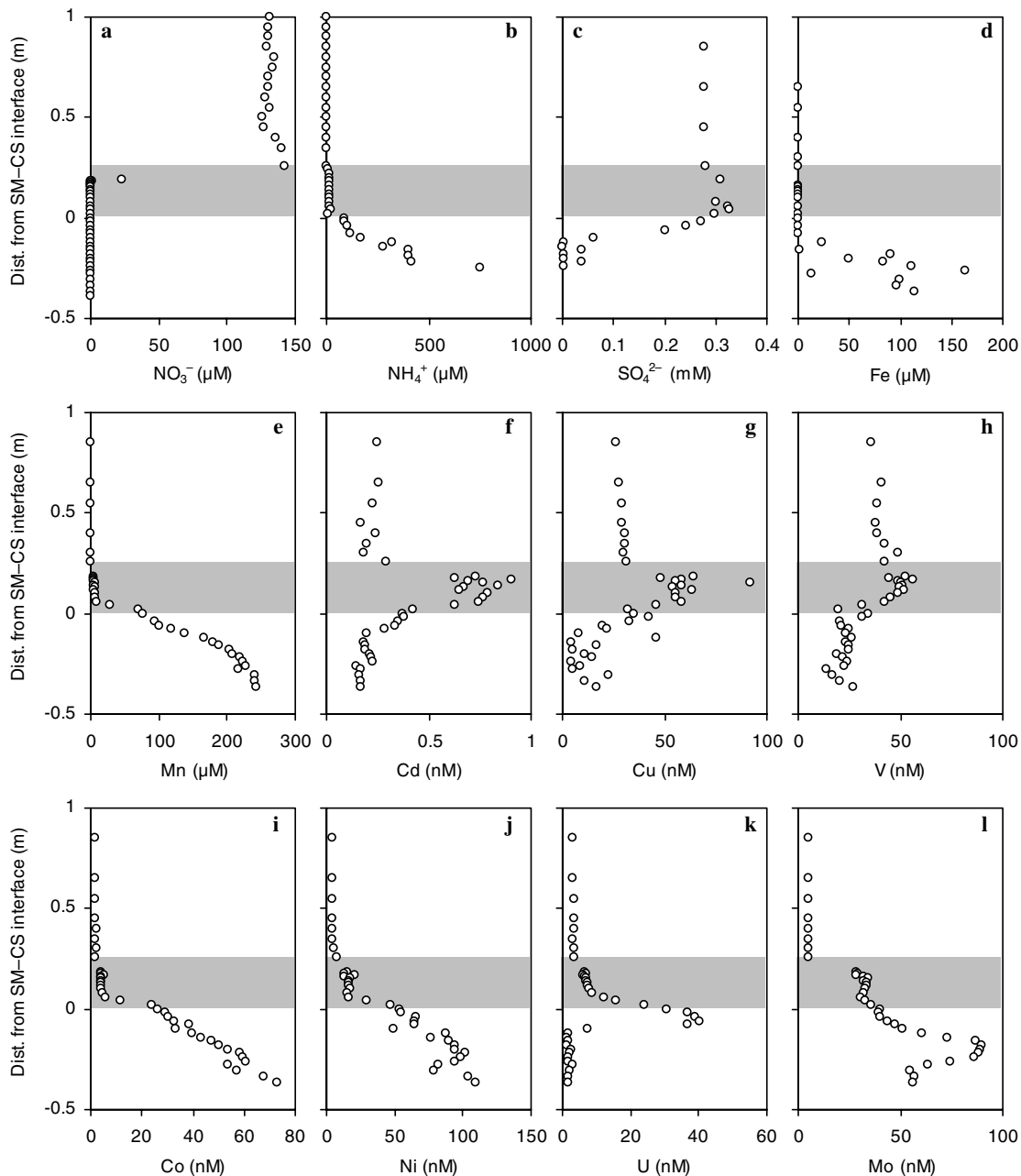
Fig. 9. Concentration–depth profiles for N-species (a and b), sulfate (c), Fe and Mn (d and e) and trace metals (f–l) at spring tide-high tide. The soft mud layer (grey area) is 25-cm thick.

3.4. Nonsteady-state diagenesis

The WC–CS system of the Gironde Estuary is characterized by density layers which function at different time-scales, consisting of two mobile zones (the LM and the SM layers) overlying more consolidated sediments (Fig. 2). This results in a three-zone diagenetic regime where sediment–water exchange, resetting of reaction conditions, redox oscillations and reoxidation processes are enhanced in the mobile layers. The mobile layers can be chemically considered as unsteady batch reactors which diagenetic properties depending on the relative

scaling of reaction rates and transport dimensions (Aller, 2004).

The sporadic presence of NO_3^- in the anaerobic part of the cores (Figs. 6a–8a) testifies to important reoxidation processes in the anoxic sediment. The small NO_3^- peak (~4 μM) in the SM (7 cm below the SM–CS boundary) at neap tide-low tide (Fig. 6a) is likely due to NH_4^+ oxidation to NO_3^- (i.e., anoxic nitrification) by Mn oxides (Aller and Rude, 1988; Hulth et al., 1999; Anschutz et al., 2000), which is particularly in agreement with the NH_4^+ decrease (from 83 to 74 μM) observed just below the SM–CS boundary for neap tide-low tide (Fig. 6b).
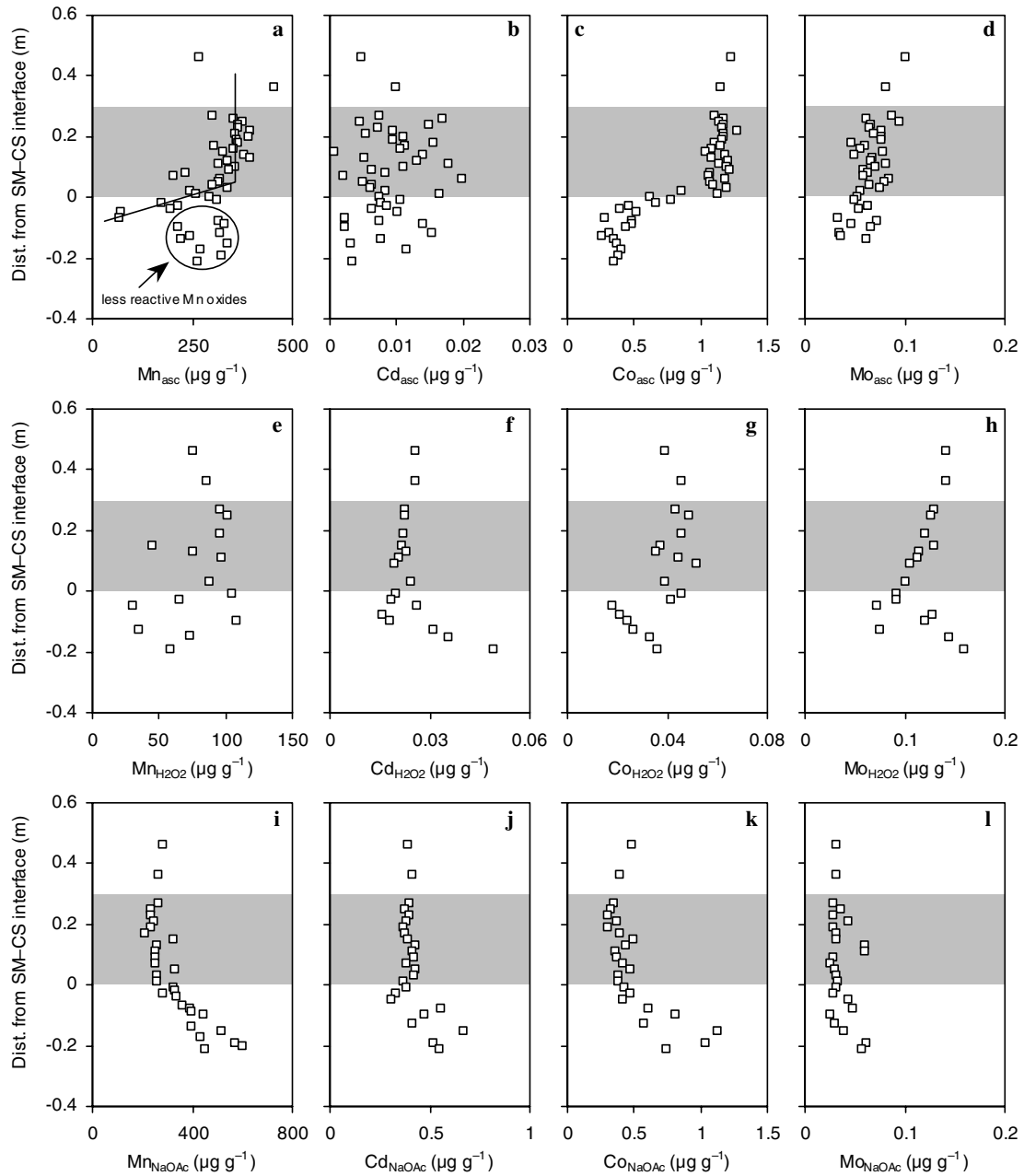
Fig. 10. Concentration–depth profiles of Mn, Cd, Co, and Mo in the solid fractions selectively extracted (see Table 1 for details) from the core of the neap tide-high tide situation.

However, the NO_3^- peak for neap tide-high tide (6.9 μM; Fig. 7a) at 8 cm above the SM–CS boundary cannot be attributed to anoxic nitrification via Mn/Fe oxide reduction as (1) this process should also produce dissolved Fe and/or Mn, which is not observed at this depth range, and (2) NH_4^+ is not detectable in this depth range (Figs. 7b and e). Thus, this NO_3^- peak is rather attributed to a lateral sliding of SM from zones adjacent to the sampling point, where the SM is not totally NO_3^- depleted and reductive dissolution of Mn oxides does not occur. This interpretation of the data is supported by the thicker SM observed for neap tide-high tide (30 cm) compared to neap tide-low tide (15 cm). The fact that this NO_3^-

peak is no longer observed for spring tide-high tide indicates again that redox processes occurring in the SM are highly transient. Furthermore, the low and nearly constant dissolved Mn concentrations (∼6 μM) observed in the SM for spring tide (Figs. 8e and 9e) are likely due to partial SM resuspension between neap tide and spring tide and indicate redox oscillations and the occurrence of transient redox processes in the SM.

3.5. Trace metal behavior during early diagenesis

Trace metals in the fluvial Gironde Estuary turbidity layers are affected by multiple and complex early diagenetic
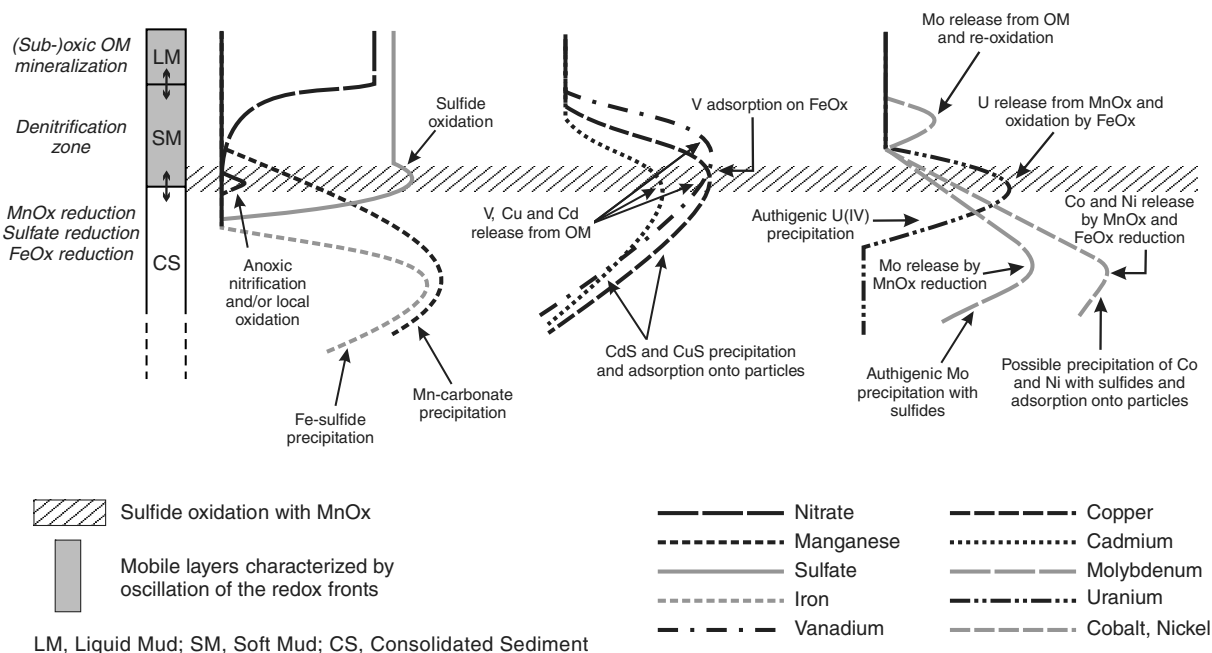
Fig. 11. Schematic conceptual model of the three-zone diagenetic regime of the sediments of the Gironde Estuary's fluvial reaches summarizing the transient behaviors of selected trace metals. The profiles show the evolution of dissolved major redox species and metals as a function of depth.

processes, as schematically presented in the conceptual model presented in Fig. 11. For all four tidal situations, dissolved trace metal concentrations in the LM are relatively constant, with values of about 0.2 nM (Cd), 2 nM (Co), 4 nM (Ni and U), 5 nM (Mo), 30 nM (Cu), and 40 nM (V) indicating no release or removal in this layer (Figs. 6–9). Deeper, peaks suggesting release of dissolved trace metals occur in distinct zones in the SM–CS system.

3.5.1. Cadmium, copper, and vanadium

Cadmium, Cu, and V concentrations increase in the denitrification zone, at the depth where dissolved Mn and Fe are still below the detection limit, and reach maximum concentrations in the SM (Figs. 6–9f–h). This distribution suggests that Cd, Cu, and V are principally released from biogenic material in the upper part of the profiles by degradation of OM which is intense in this zone (Abril et al., 1999, 2000; Robert et al., 2004). This interpretation is supported by the solid phase data that show, for example, Cd associated with the H_2O_2-extracted fraction ($Cd_{H_2O_2}$) decreasing just below the LM–SM boundary, while Cd extracted by the ascorbate leaching (Cd_{asc}) shows no particular trend (Figs. 10b and f). The release of dissolved Cd and Cu in the SM due to OM mineralization is in agreement with previous work reporting similar observations at the water–sediment interface of various marine environments (e.g., Klinkhammer et al., 1982; Gendron et al., 1986; Gobeil et al., 1987; Widerlund, 1996). While V behavior is less documented, association of this metal with OM has been reported in marine (Emerson and Huested, 1991) and estuarine (Shiller and Boyle, 1987) environ-

ments. Interestingly, the profiles of Cd, Cu, and V for neap tide-low tide imply a sequence where V is mobilized first in the upper SM, then Cu, followed by Cd near the SM–CS boundary (Figs. 6f–h). The redox conditions become more and more reducing from the LM to the SM, as shown by the fast decrease of O_2 (Fig. 5) and the onset of denitrification (Fig. 6a). Therefore, the observed sequence of metal release could be related to the binding strength to OM that would follow the order Cd > Cu > V. However, this contention is not supported by the results of Tipping and Hurley (1992) who found the binding strength of metals to OM (humic substances) to increase in the order Cd < Cu < V. An alternative explanation could be that V, Cu, and Cd were associated with OM characterized by different lability: V, which is released first, being released from more labile OM than Cd, which is released last. However, further investigations on OM characterization are needed to resolve this particular observation.

Dissolved Cd, Cu, and V peaks observed for spring tide are similar or even higher than those at neap tide (Figs. 6–9). Assuming probable (partial) resuspension of the SM during neap tide-spring tide cycles, the observed concentration gradients due to trace metal release in this layer may be installed at a weekly to monthly time-scale.

Removal of Cd and Cu from pore water occurs in the sulfate reduction zone (Figs. 6–9f and g). This removal comes along with increasing concentrations of both metals extracted by the H_2O_2 leaching, as shown for example for Cd in Fig. 10f. The H_2O_2 leaching does not permit distinguishing between organically bound and sulfide-bound metals (Gleyses et al., 2002). Nevertheless, an increase in

metal concentration extracted by H_2O_2 can hardly be attributed to organic-bound metal since the amount of trace metal associated with particulate organics is likely to decrease with depth due to OM degradation (Allen et al., 1990). Therefore, these observations strongly suggest metal precipitation with sulfide. Phases as CdS and CuS, rather than coprecipitation with Fe sulfides, are likely to form due to the strong affinity of these metals for sulfide (Öztürk, 1995; Zwolsman et al., 1997) and given that Cd and Cu have faster water exchange reaction kinetics than Fe^{2+} resulting in metal-sulfide phase precipitation prior to FeS formation (Morse and Luher, 1999). Moreover, CdS precipitation was shown to occur in the presence of very low dissolved sulfide concentrations (Lapp and Balzer, 1993; Morford and Emerson, 1999). However, reactive Mn oxides (extracted by the ascorbate solution) are still present at depth in the CS (Fig. 10a). Therefore, sorption of Cd on Fe/Mn oxides could explain part of the Cd removal from solution (e.g., Trefy and Metz, 1989; Morford and Emerson, 1999). It seems that the initial V decrease in the SM or at the SM–CS boundary (Figs. 6h–9h) coincides with Fe cycling, i.e., V first adsorbs to Fe oxides (Auger et al., 1999; Peacock and Sherman, 2004) then is removed in the sulfate-reduction zone.

An important point is that, while the Cd, Cu, and V behaviors in the SM are certainly driven by OM mineralization, reoxidation of these metals in the SM evidently modifies these initial behaviors. This is not surprising given the physically dynamic nature of the SM (Abril et al., 1999; Robert et al., 2004), which is particularly shown by the NO_3^- peaks in the anoxic SM reflecting the onset of changed diagenetic conditions (i.e., migration of redox fronts) and by the SO_4^{2-} production reflecting reoxidation processes within this zone. As a consequence, Cd, Cu, and V probably undergo successive and repeated reduction-oxidation cycles within the SM resulting in scattered profiles for the dissolved concentrations of these metals for neap tide-high tide and spring tide-low tide (Figs. 7 and 8).

3.5.2. Cobalt, nickel, uranium, and molybdenum

The release of Co and Ni in the pore water occurs deeper than that of V, Cu and Cd, i.e., in the CS and concomitantly to the reductive dissolution of Mn oxides (Figs. 6 and 7). This strongly suggests that Co and Ni are delivered to the sediment mainly associated with Mn oxides and released from these particles to the pore water when Mn oxides are reduced during OM mineralization. This point is supported by the solid data that show, for example, a clear decrease of Co_{asc} (from 1.1 to 0.26 $\mu g\,g^{-1}$; Fig. 10c) at the SM–CS boundary. This point is also in agreement with previous work reporting, for various estuarine and marine sediments, association of these metals with Mn oxides, e.g., Gendron et al. (1986); Lewis and Landing (1992); Zwolsman and Van Eck (1999) for Co, and Shaw et al. (1990) for Co and Ni. Moreover, additional release of Co and Ni at depth could be supplied by reduction of

Fe oxides that were shown to be important transport phases for these metals (Douglas and Adeney, 2000; Gunnarsson et al., 2000). In contrast to trace metals preferentially released from OM (i.e., Cd, Cu, and V), Co and Ni are not removed from solution to the depth sampled as shown by the strong and still increasing dissolved concentration gradients in the CS (Figs. 6, 8, and 9). This is less true for neap tide-high tide given the scatter of the dissolved Co and Ni data (Figs. 7i and j) that suggests possible precipitation with sulfides, which is supported, for example, by the slight increase of $Co_{H_2O_2}$ in the CS (Fig. 10g). Association of Co and Ni with authigenic Fe sulfides were reported in estuarine (Luther et al., 1980) and fjord sediments (Öztürk, 1995). However, there is no significant relationship between dissolved Co, Ni, and Fe concentrations that could denote co-precipitation of Co and Ni with iron sulfides in the Gironde Estuary freshwater sediments. Therefore, Co and Ni probably undergo authigenic precipitation as CoS and NiS, which is in agreement with observations reported by Kremling (1983) and Huerta-Diaz et al. (1998).

An interesting aspect of this data set is that, while U is supposed to be insoluble under anoxic conditions, dissolved U is present in the SM and CS for all four tidal situations (Figs. 6k–9k). Uranium release in pore water occurs in the CS where dissolved Mn increases drastically, suggesting that U is released from Mn oxides in the upper part of the CS and likely from both Mn and Fe oxides deeper in the CS. This explanation is entirely in agreement with the work of Barnes and Cochran (1993). From both estuarine sediment pore water profiles and incubation experiments, these authors showed the presence of dissolved U peaks in the anoxic sediment and concluded to the release of U from Mn and Fe oxides during reductive dissolution. The occurrence of dissolved U in anoxic sediment was previously reported by numerous studies (e.g., Zhorov et al., 1982; Cochran et al., 1986; Chaillou et al., 2002). In most cases, authors attributed the presence of dissolved U in anoxic sediment to sampling artifacts due to (1) re-oxygenation of the sediment during core slicing inducing conversion of particulate U(IV) to dissolved U(VI) (e.g., Anderson et al., 1989), or (2) possible presence of authigenic colloidal phases in the dissolved phase that could cross the 0.2 μm pore size filters (Chaillou et al., 2002). While we cannot totally exclude the presence of colloidal U in the pore water, it seems unlikely that this artifact could explain the observed well-defined increasing gradient of dissolved U. Hence, the persistence of U(VI) in the anoxic SM and CS of the Gironde Estuary is attributed to oxidation by Fe(III) (Sani et al., 2004) present as Fe oxides in the SM and the upper part of the CS. The substantial decrease of dissolved U in pore water to constant concentrations of 1–2 nM, corresponding to a removal of more than 90% of the U previously released, is accomplished at depth where sulfate is totally depleted and in the zone of the reductive dissolution of Fe oxides (Figs. 6–9). This indicates authigenic U formation in the CS,

and suggests a coupling of Fe(III) and U(VI) reduction (Zheng et al., 2002).

Uranium reduction has been shown to occur via both microbial (e.g., Lovley et al., 1991; Tebo and Obraztsova, 1998; Fredrickson et al., 2000; Gu and Chen, 2003) and abiotic pathways (Wersin et al., 1994; Liger et al., 1999; Behrends and Van Cappellen, 2005). The Fe(III)/U(VI) ratio has been proposed to be the master parameter controlling the dominant U reduction pathway: high Fe(III)/U(VI) ratio favors the abiotic pathway (Fe(III) > 10 mM and U(VI) < 0.5 μM; Behrends and Van Cappellen, 2005) while low Fe(III)/U(VI) ratio favors the microbial pathway (Wielinga et al., 2000). In the CS of the Gironde Estuary, Fe(III)/U(VI) ratios are high, i.e., Fe(III) > 0.8 mM (Fe$_{asc}$; see above) and U(VI) < 40 nM, suggesting that abiotic reduction of U(VI) by Fe(II) could outcompete the microbial pathway. Microbially mediated enzymatic U(VI) reduction can be achieved by either dissimilatory sulfate-reducing (Sani et al., 2004) or metal-reducing bacteria (Fredrickson et al., 2000). If microbially mediated U(VI) reduction takes place in the Gironde Estuary sediments, it is likely that the metal-reducing pathway is the one favored as authigenic precipitation of U(IV) occurs at depth where sulfate is totally consumed, i.e., where the main microbial activity should be related to metal-reducing bacteria (as suggested by increasing dissolved Mn and Fe concentrations).

Molybdenum release occurs in the zone of the reductive dissolution of Mn oxides (Figs. 6–9). Dissolved Mo concentrations show a peak in the CS, at depth where sulfate is totally depleted and dissolved Mn concentrations still increase. Obviously, at least one component of Mo co-cycles with Mn in the Gironde Estuary sediments. Molybdate (MoO$_4^{2-}$), the soluble form of Mo in oxic water, is probably adsorbed onto Mn oxides (Shimmield and Price, 1986; Calvert and Pedersen, 1993). Hence, Mo is likely released into pore water when Mn oxides dissolve (Malcolm, 1985), which seems to be confirmed by the slightly decreasing Mo$_{asc}$ concentrations in the lower part of the SM (Fig. 10d). An aspect that distinguishes Mo behavior from those of Co and Ni is that Mo shows a peak of dissolved concentrations (14.7 nM) in the SM (neap tide-high tide; Fig. 7l), i.e., in the denitrification zone and above the zone of Mn oxide reduction. This observation and the decrease of Mo extracted by H$_2$O$_2$ Mo$_{H_2O_2}$ in the SM (from 0.14 to 0.10 μg g^{-1}; Fig. 10h), strongly suggest that some Mo is released from OM by organic carbon mineralization. This interpretation is in agreement with the reported affinity of Mo for OM (Malcolm, 1985) in estuarine sediment, and with the results of Shaw et al. (1990). At the bottom of the cores, Mo removal represents from 15% (neap tide-low tide) to 50% (neap tide-high tide) of the Mo previously released and the strongest removals are observed for the cores with highest dissolved Fe in the CS (Figs. 7 and 9). Particulate total Mo concentrations increase (from 0.38 to 1.37 μg g^{-1}; Fig. 4h) in

the CS. All these observations combined together indicate anoxic Mo authigenesis and local accumulation in the CS. The H$_2$O$_2$ leaching data show an increase of Mo$_{H_2O_2}$ in the CS (Fig. 10h), suggesting that at least part of Mo is removed from solution by precipitation with authigenic sulfide phases, as previously reported by Pedersen (1985); Shaw et al. (1990); Adelson et al. (2001) for coastal and continental margin sediments and by Erickson and Helz (2000) in laboratory experiments. Molybdenum can be trapped with reduced sulfur forming Mo–Fe–S by co-precipitation or directly by MoS$_2$ or MoS$_3$ precipitation (e.g., Chaillou et al., 2002). Zheng et al. (2000) found apparent sulfide thresholds of 0.1 μM for the onset of the co-precipitation of Mo with iron-sulfide phases and of ∼100 μM for the onset of Mo precipitation without Fe. We have estimated earlier that the potentially dissolved sulfide produced by sulfate reduction is 3 mM and that 20% of this amount may be oxidized back to sulfate. Taking into account that 0.8 mM of dissolved Fe may potentially react with dissolved sulfides in the CS, we roughly estimate that the dissolved sulfides remaining for precipitation with Mo should be one order of magnitude higher than the threshold of 100 μM. Therefore, as enhanced Mo removal is observed in depth with high Fe concentrations, both direct Mo–S precipitation and co-precipitation of Mo–Fe–S might co-exist in the CS. In the SM, the diagenetically controlled distributions of Co, Ni, U, and Mo described above are probably influenced by nonsteady-state processes, i.e., oscillations of oxidation fronts. This is suggested by the constant or slightly increasing concentrations of Co, Ni, and U in the SM for spring tide above the sharply increasing concentration gradients in the CS related to release from Mn and Fe oxides (Figs. 8 and 9). Cobalt, Ni and U are released in the CS and diffuse upward through the SM–CS boundary. It is possible that partial resuspension of the SM has resulted in homogenization of Co, Ni, and U concentration building up the unsteady profiles observed in the SM. It is also very likely that Mo is influenced by nonsteady-state processes such that authigenic Mo can be mobilized, as suggested by irregularities in dissolved Mo profiles in the SM for high tide (Figs. 7l and 9l). Such irregularities have also been observed in marine sediments (Shaw et al., 1990; Zheng et al., 2000). While OM mineralization has been designated here to mainly explain the dissolved Mo peak in the upper SM (Figs. 7l and 9l), other factors could also have contributed to Mo pore water profiles: (1) remobilisation of authigenic Mo previously formed under more reducing conditions, and/or (2) the presence of micro-zones of Mo precipitation/dissolution due to sulfate reduction and sulfide oxidation (Zheng et al., 2000). Both processes seem possible in the SM of the Gironde Estuary that is affected by repeated partial resuspension causing new material inputs and sulfide oxidation near the SM–CS boundary.

3.6. Metal sequestration in the Gironde Estuary sediments

The highly reductive conditions rapidly established in the SM prevent the recycling of Fe and Mn. Manganese is trapped by carbonate (acetate leached) phases at depth. The H_2O_2 leaching underlines trace metal trapping with sulfide phases at depth. These authigenic sulfide phases are likely characterized by low solubility, considering the low trace metal concentrations extracted by the H_2O_2 leaching (i.e., from 0.1% for V to 16% for Mo). Therefore, it is expected that the sulfide-associated metals will remain trapped in the CS. However, another part of the trace metals studied here is trapped in the CS under exchangeable form, rather than associated with carbonate as no relationship between the NaOAc-extracted fraction of the trace metals and inorganic carbon was found. Considering the dynamics of the Gironde Estuary, (i.e., strong river floods and dredging that would cause sediment remobilization), the metals trapped under exchangeable forms could be mobilized by changed (oxidizing) redox conditions. The exchangeable part of the trace metals could constitute the dominant part of the reactive (i.e., nonresidual) metals, as suggested by the higher trace metal concentrations in the NaOAc-extracted fraction compared to the H_2O_2-extracted fraction. Nevertheless, selectivity problems may have artificially enhanced the proportion of trace metals associated with the exchangeable fraction, and the amounts of trace metal associated with sulfides are probably higher than given here, as H_2O_2 leaching extracts only the most amorphous sulfide phases (Gleyses et al., 2002).

4. Conclusion

1. The water column-consolidated sediment system of the freshwater Gironde Estuary is characterized by a three-zone diagenetic regime due to the superposition of density layers functioning at different time-scales. Oxygen consuming reactions are fast enough to produce depletion in the rapidly mixed liquid mud layer (tidal time-scale); nitrate consumption proceeds in the soft mud layer (weekly time-scale); the Mn, Fe, and sulfate cycling occurs in the consolidated sediment layer (annual time-scale).
2. Trace metals show differential behaviors during early diagenesis: (1) Cd, Cu, and V are suggested to be preferentially released into the pore water from organic matter, (2) Co, Ni, and U from Mn and Fe oxides and (3) Mo from both organic matter and Mn and Fe oxides.
3. Nonsteady-state processes (i.e., oscillations of redox fronts), due to partial resuspension of the soft mud layer and lateral soft mud inputs, exert strong influence on the trace metal distributions, causing trace metal mobilization, particularly for Cd, Cu, and Mo.
4. In the consolidated sediment, Mn is trapped as carbonate and Fe is associated with sulfides. Trace metals (except Co and Ni) are removed from solution partly associated with sulfides, either likely by direct precipitation (Cu, Cd) or co-precipitation with Fe-sulfides (Mo). Iron and U cycles appear tightly connected, as microbially mediated reduction of Fe oxides is thought to control the reduction of U(VI) to U(IV) at depth.
5. An important part of the trace metals is trapped in the sediment under exchangeable form. This and the fact that relatively small changes in ambient chemical conditions (e.g., pH, Eh, O_2 concentrations, etc.) could change the particulate metal speciation in the estuarine sediment, suggest that trace metals trapped in the Gironde Estuary sediment should not be considered as immobile. Therefore, as remobilization of estuarine sediment is probable, due to erosion during river floods or dredging, mobilization of trace metals from the solid phase to the water column remains possible.

Appendix A. Supplementary data

Supplementary data associated with this article can be found, in the online version, at doi:10.1016/j.gca.2006.02.001.

References

Abril, G., Etcheber, H., Le Hir, P., Bassoulet, P., Boutier, B., Frankignoulle, M., 1999. Oxic/anoxic oscillations and organic carbon mineralization in an estuarine maximum turbidity zone (The Gironde, France). *Limnol. Oceanogr.* **44**, 1304–1315.
Abril, G., Riou, S.A., Etcheber, H., Frankignoulle, M., de Wit, R., Middelburg, J.J., 2000. Transient, tidal time-scale, nitrogen transformations in an estuarine turbidity maximum-fluid mud system (The Gironde, South-West France). *Estuar. Coast. Shelf Sci.* **50**, 703–715.
Adelson, J.M., Helz, G.R., Miller, C.V., 2001. Reconstructing the rise of recent coastal anoxia: molybdenum in Chesapeake bay sediments. *Geochim. Cosmochim. Acta* **65**, 237–252.
AFNOR, 1996. NF ISO 10304-2. Dosage d'ions (F⁻, Cl⁻, NO₂⁻, NO₃⁻, Br⁻, PO₄³⁻ et SO₄²⁻ par chromatographie des ions en phase liquide. Partie 1: Méthode applicable pour les eaux usées. 3, 171–196. ISBN 2-12-179020-9 (second ed.).
Alborés, A.F., Cid, B.P., Gómez, E.F., López, E.F., 2000. Comparison between sequential extraction procedures and single extractions for metal partitioning in sewage sludge samples. *Analyst* **125**, 1353–1357.
Allen, G.P., Sauzay, G., Castaing, P., Jouanneau, J.M., 1977. Transport and deposition of suspended sediment in the Gironde Estuary, France.

In: Wiley, M. (Ed.), *Estuarine Processes*. Academic Press, New York, pp. 63–81.

Allen, J.R., Rae, J.E., Zanin, P.E., 1990. Metal speciation (Cu, Zn and Pb) and organic matter in an oxic salt marsh, Seven Estuary, Southwest Britain. *Mar. Poll. Bull.* **21**, 574–580.

Aller, R.C., Rude, P.D., 1988. Complete oxidation of solid phase sulfides by manganese and bacteria in anoxic marine sediments. *Geochim. Cosmochim. Acta* **52**, 751–765.

Aller, R.C., 2004. Conceptual models of early diagenetic processes: the muddy seafloor as an unsteady, batch reactor. *J. Mar. Res.* **62**, 815–835.

Anderson, L., 1979. Simultaneous spectrophotometric determination of nitrite and nitrate by flow injection analysis. *Anal. Chim. Acta* **110**, 123–128.

Anderson, R.F., Le Huray, A.P., Fleisher, M.Q., Murray, J.W., 1989. Uranium deposition in Saanich Inlet sediments, Vancouver Island. *Geochim. Cosmochim. Acta* **53**, 2205–2213.

Anschutz, P., Sundby, B., Lefrancois, L., Luther III, G.W., Mucci, A., 2000. Interactions between metal oxides and species of nitrogen and iodine in bioturbated marine sediments. *Geochim. Cosmochim. Acta* **64**, 2751–2763.

Anschutz, P., Zhong, S., Sundby, B., Mucci, A., Gobeil, C., 1998. Burial efficiency of phosphorus and the geochemistry of iron in continental margin sediments. *Limnol. Oceanogr.* **43**, 53–64.

Audry, S., Blanc, G., Schäfer, J., 2004. Cadmium transport in the Lot-Garonne River system (France)—temporal variability and a model for flux estimation. *Sci. Total Environ.* **319**, 197–213.

Auger, Y., Bodineau, L., Leclercq, S., 1999. Some aspects of vanadium and chromium chemistry in the English Channel. *Cont. Shelf Res.* **19**, 2003–2018.

Barnes, C.E., Cochran, J.K., 1993. Uranium geochemistry in estuarine sediments: control on removal and release processes. *Geochim. Cosmochim. Acta* **57**, 555–569.

Bassoulet, P., Le Hir, P., 1997. Mesures hydrosédimentaires in-situ dans l'entité bouchon vaseux-crème de vase. IFREMER-UMR13, Internal Report, pp. 93–108.

Blanc, G., Lapaquellerie, Y., Maillet, N., Anschutz, P., 1999. A cadmium budget for the Lot-Garonne fluvial system (France). *Hydrobiologia* **410**, 331–341.

Behrends, T., Van Cappellen, P., 2005. Competition between enzymatic and abiotic reduction of uranium(VI) under iron reducing conditions. *Chem. Geol.* **220**, 315–327.

Boesen, C., Postma, D., 1988. Pyrite formation in anoxic environments of the Baltic. *Am. J. Sci.* **288**, 575–603.

Böttcher, M.E., Thamdrup, B., 2001. Anaerobic sulfide oxidation and stable isotope fractionation associated with bacterial sulfur disproportionation in the presence of MnO_2. *Geochim. Cosmochim. Acta* **65**, 1573–1581.

Boutier, B., 1981. Synthèse des résultats de la surveillance des micropolluants dans la matière vivante. Ministère de l'Environnement. *Bulletin du Réseau National d'Observation* **17**, 115–174.

Burdige, D.J., 1993. The biogeochemistry of manganese and iron reduction in marine sediments. *Earth Sci. Rev.* **35**, 249–284.

Calvert, S.E., Pedersen, T.F., 1993. Geochemistry of recent and anoxic marine sediments: Implication for the geological records. *Mar. Geol.* **113**, 67–88.

Canfield, D.E., 1989. Reactive iron in marine sediments. *Geochim. Cosmochim. Acta* **53**, 619–632.

Canfield, D.E., 1993. Organic matter oxidation in marine sediments. In: Wollast, R., Mackenzie, F.T., Chou, L. (Eds). Interactions of C, N, P and S Biogeochemical Cycles and Global Change. NATO ASI Series vol. 14, pp. 333–363.

Castaing, P., 1981. Le transfert à l'océan des suspensions estuariennes. Cas de la Gironde. State Thesis dissertation, Univ. Bordeaux 1, p. 530.

Cauwet, G., Gadel, F., de Souza Sierra, M.M., Donard, O.F.X., Ewald, M., 1990. Contribution of the Rhône river to organic carbon inputs to the Northwestern Mediterranean Sea. *Cont. Shelf Res.* **10**, 1025–1037.

Chadwell, S.J., Rickard, D., Luther, G.W., 1999. Electrochemical evidence for pentasulfide complexes with Mn^{2+}, Fe^{2+}, Co^{2+}, Ni^{2+}, Cu^{2+} and Zn $^{2+}$. *Aquat. Geochem.* **5**, 29–57.

Chadwell, S.J., Rickard, D., Luther, G.W., 2000. Electrochemical evidence for metal polysulfide complexes: tetrasulfide (S_4^{2-}) reactions with Mn^{2+}, Fe^{2+}, Co^{2+}, Ni^{2+}, Cu^{2+} and Zn^{2+}. *Electroanalysis* **13**, 21–29.

Chaillou, G., Anschutz, P., Lavaux, G., Schäfer, J., Blanc, G., 2002. The distribution of Mo, U, and Cd in relation to major redox species in muddy sediments of the Bay of Biscay. *Mar. Chem.* **80**, 41–59.

Chiffoleau, J.F., Cossa, D., Auger, D., Truquet, I., 1994. Trace metal distribution, partition and fluxes in the Seine estuary (France) in low discharge regime. *Mar. Chem.* **47**, 145–158.

Cochran, J.K., Carey, A.E., Sholkovitz, E.R., Surprenant, L.D., 1986. The geochemistry of uranium and thorium in coastal marine sediments and sediment pore waters. *Geochim. Cosmochim. Acta* **50**, 663–680.

Douglas, G.B., Adeney, J.A., 2000. Diagenetic cycling of trace elements in the bottom sediments of the Swan River Estuary, Western Australia. *Appl. Geochem.* **15**, 551–566.

Elbaz-Poulichet, F., Garnier, J.M., Guan, D.M., Martin, J.M., Thomas, A.J., 1996. The conservative behavior of trace metals (Cd, Cu, Ni and Pb) and As in the surface plume of stratified estuaries: example of the Rhône river (France). *Estuar. Coast. Shelf Sci.* **42**, 289–310.

Emerson, S.R., Huested, S.S., 1991. Ocean anoxia and the concentrations of molybdenum and vanadium in seawater. *Mar. Chem.* **34**, 177–196.

Erickson, B.E., Helz, G.R., 2000. Molybdenum (VI) speciation in sulfidic waters: stability and lability of thiomolybdates. *Geochim. Cosmochim. Acta* **64**, 1149–1158.

Fredrickson, J.K., Zachara, J.M., Kennedy, D.W., Duff, M.C., Gorby, Y.A., Li, S.W., Krupka, K.M., 2000. Reduction of U(VI) in goethite (α-FeOOH) suspensions by dissimilatory metal-reducing bacterium. *Geochim. Cosmochim. Acta* **64**, 3085–3098.

Froelich, P.N., Klinkhammer, G.P., Bender, M.L., Luedtke, N.A., Heath, G.R., Cullen, D., Dauphin, P., Hammond, D., Hartman, B., Maynard, V., 1979. Early oxidation of organic matter in pelagic sediments of the Eastern Equatorial Atlantic: suboxic diagenesis. *Geochim. Cosmochim. Acta* **43**, 1075–1090.

Gendron, A., Silverberg, N., Sundby, B., Lebel, J., 1986. Early diagenesis of cadmium and cobalt in sediments of the Laurentian Trough. *Geochim. Cosmochim. Acta* **50**, 741–747.

Gleyses, C., Tellier, S., Astruc, M., 2002. Fractionation studies of trace elements in contaminated soils and sediments: a review of sequential extraction procedures. *Trends Anal. Chem.* **21**, 451–467.

Gobeil, C., Silverberg, N., Sundby, B., Cossa, D., 1987. Cadmium diagenesis in Laurentian trough sediments. *Geochim. Cosmochim. Acta* **51**, 589–596.

Grousset, F., Jouanneau, J.M., Castaing, P., Lavaux, G., Latouche, C., 1999. A 70 year record of contamination from industrial activity along the Garonne River and its tributaries (SW France. Estuar) Coast. *Shelf Sci.* **48**, 401–414.

Gu, B., Chen, J., 2003. Enhanced microbial reduction of Cr(VI) and U(VI) by different natural organic matter fractions. *Geochim. Cosmochim. Acta* **67**, 3575–3582.

Guieu, C., Martin, J.M., Tankere, S.P.C., Mousty, F., Trincherini, P., Bazot, M., Dai, M.H., 1998. On trace metal geochemistry in the Danube river and Western Black sea. *Estuar. Coast. Shelf Sci.* **47**, 471–485.

Gunnarsson, M., Jakobsson, A.-M., Ekberg, S., Albinsson, Y., Ahlberg, E., 2000. Sorption studies of cobalt(II) on colloidal hematite using potentiometry and radioactive tracer technique. *J. Colloid Interface Sci.* **231**, 326–336.

Hall, P.O.J., Aller, R.C., 1992. Rapid, small-volume flow injection analysis for CO_2 and NH_4^+ in marine and fresh waters. *Limnol. Oceanogr.* **37**, 1113–1119.

Huerta-Diaz, M.A., Tessier, A., Carignan, R., 1998. Geochemistry of trace metals associated with reduced sulfur in freshwater sediments. *Appl. Geochem.* **13**, 213–233.

Hulth, S., Aller, R.C., Gibert, F., 1999. Coupled anoxic nitrification/manganese reduction in marine sediments. *Geochim. Cosmochim. Acta* **63**, 49–66.

Jouanneau, J.M., Latouche, C., 1981. The Gironde Estuary. In: Fürchtbauer, H., Lisitzyn, A.P., Millerman, J.D., Seibold, E. (Eds.) *Contribution to Sedimentology*. vol. 10, Stuttgart, pp. 1–115.

Klinkhammer, D., Heggie, D.T., Graham, D.W., 1982. Metal diagenesis in oxic marine sediments. *Earth Planet. Sci. Lett.* **61**, 211–219.

Kostka, J.E., Luther III, G.W., 1994. Partitioning and speciation of solid phase iron in saltmarsh sediments. *Geochim. Cosmochim. Acta* **58**, 1701–1710.

Kraepiel, A.M.L., Chiffoleau, J.F., Martin, J.M., Morel, F.M.M., 1997. Geochemistry of trace metals in the Gironde estuary. *Geochim. Cosmochim. Acta* **61**, 1421–1436.

Kremling, K., 1983. The behavior of Zn, Cd, Cu, Ni, Co, Fe, and Mn in anoxic baltic waters. *Mar. Chem.* **13**, 87–108.

Lapp, B., Balzer, W., 1993. Early diagenesis of trace metals used as an indicator of past productivity changes in coastal sediments. *Geochim. Cosmochim. Acta* **57**, 4639–4652.

Lasslet, R.E., Balls, P.W., 1995. The behaviour of dissolved Mn, Ni and Zn in the Forth, an industrialized, partially mixed estuary. *Mar. Chem.* **48**, 311–328.

Latouche, C., 1988. Cadmium pollution in the Gironde estuary. *Bulletin de l'institut Géologique du Bassin d'Aquitaine, Bordeaux* **44**, 15–21.

Latouche, C., 1992. La pollution par le cadmium des huîtres sauvages de l'Estuaire de la Gironde. Origine. Mécanismes responsables de la fixation du cadmium. *Ichtyophysiol. Acta* **15**, 139–152.

Lewis, B.L., Landing, W.M., 1992. The investigation of dissolved and suspended-particulate trace metal fractionation in the Black Sea. *Deep Sea Res.* **38** (Suppl.), S773–S803.

Liger, E., Charlet, L., van Cappellen, P., 1999. Surface catalysis of uranium (VI) reduction by iron (II). *Geochim. Cosmochim. Acta* **63**, 2939–2955.

Lovley, D.R., Phillips, E.J.P., Gorby, Y.A., Landa, E.R., 1991. Microbial reduction of uranium. *Nature* **350**, 413–416.

Luther, G.W., Meyerson, A.L., Krajewski, J.J., Hires, R., 1980. Metal sulfides in estuarine sediments. *J. Sediment. Petrol.* **50**, 1117–1120.

Luther III, G.W., Ferdelman, T.G., 1993. Voltammetric characterization of iron (II) sulfide complexes in laboratory solutions and in marine waters and porewaters. *Environ. Sci. Technol.* **27**, 1154–1163.

Ma, Y., Uren, N.C., 1995. Application of a new fractionation scheme for heavy metals in soils. *Commun. Soil Sci. Plant. Anal.* **26**, 3291–3303.

Malcolm, S.J., 1985. Early diagenesis of molybdenum in estuarine sediments. *Mar. Chem.* **16**, 213–225.

Martin, J.-M., Nirel, P., Thomas, A.J., 1987. Sequential extraction techniques: promises and problems. *Mar. Chem.* **22**, 313–341.

Morford, J.L., Emerson, S., 1999. The geochemistry of redox sensitive trace metals in sediments. *Geochim. Cosmochim. Acta* **63**, 1735–1750.

Morris, A.W., Bale, A.J., Howland, R.J.M., 1982. The dynamics of estuarine manganese cycling. *Estuar. Coast. Shelf Sci.* **14**, 175–192.

Morse, J.W., Luher III, G.W., 1999. Chemical influences on trace metal-sulfide interactions in anoxic sediments. *Geochim. Cosmochim. Acta* **63**, 3373–3378.

Öztürk, M., 1995. Trends of trace metals (Mn, Fe, Co, Ni, Cu, Zn, Cd and Pb) distributions at the oxic-anoxic interface and in sulfidic water of the Drammensfjord. *Mar. Chem.* **48**, 329–342.

Peacock, C.L., Sherman, D.M., 2004. Vanadium (V) adsorption onto goethite (α-FeOOH) at pH 1.5 to 12: a surface complexation model based on ad initio molecular geometries and EXAFS spectroscopy. *Geochim. Cosmochim. Acta* **68**, 1723–1733.

Pedersen, T.F., 1985. Early diagenesis of copper and molybdenum in mine tailings and natural sediments in Rupert and Holberg inlets, British Columbia. *Can. J. Earth Sci.* **22**, 1474–1484.

Postma, D., Jakobsen, R., 1996. Redox zonation: Equilibrium constraints on the Fe(III)/SO$_4^{2-}$ reduction interface. *Geochim. Cosmochim. Acta* **60**, 3169–3175.

Poulton, S.W., 2003. Sulfide oxidation and iron dissolution kinetics during the reaction of dissolved sulfide with ferrihydrite. *Chem. Geol.* **202**, 79–94.

Quevauviller, P., 1998. *Method Performance Studies for Speciation Analysis*. Royal Society of Chemistry, Cambridge, UK.

Rickard, D., 1995. Kinetics of FeS precipitation: Part 1. Competing reaction mechanisms. *Geochim. Cosmochim. Acta* **59**, 4367–4379.

Robert, S., Blanc, G., Schäfer, J., Lavaux, G., Abril, G., 2004. Metal mobilization in the Gironde Estuary (France): the role of the soft mud layer in the maximum turbidity zone. *Mar. Chem.* **87**, 1–13.

Rosenberg, E., Ariese, F., 2001. Quality control in speciation analysis. In: Ebdon, L., Pitts, L, Cornelis, R., Crews, H., Donard, O.F.X., Quevauviller, P.H. (Eds.), *Trace Element Speciation for Environment, Food and Health*. The Royal Society of Chemistry, Cambridge, UK, Chapter 6, pp. 17–50.

Rosenthal, Y., Lam, P., Boyle, E.A., Thomson, J., 1995. Authigenic cadmium enrichment in suboxic sediments: Precipitation and postdepositional mobility. *Earth Planet. Sci. Lett.* **132**, 99–111.

Sani, R.K., Peyton, B.M., Amonette, J.E., Geesey, G.G., 2004. Reduction of uranium(VI) under sulfate-reducing conditions in the presence of Fe(III)-(hydr)oxides. *Geochim. Cosmochim. Acta* **68**, 2639–2648.

Schäfer, J., Blanc, G., Lapaquellerie, Y., Maillet, N., Maneux, E., Etcheber, E., 2002. Ten-year-observation of the Gironde tributary fluvial system: Fluxes of suspended matter, particulate organic carbon and cadmium. *Mar. Chem.* **79**, 229–242.

Shaw, T.J., Gieskes, J.M., Jahnke, R.A., 1990. Early diagenesis in differing depositional environments: The response of transition metals in pore water. *Geochim. Cosmochim. Acta* **54**, 1233–1246.

Shiller, A.M., Boyle, E.A., 1987. Dissolved vanadium in rivers and estuaries. *Earth Planet. Sci. Lett.* **86**, 214–224.

Shink, D., 1981. Behaviour of chemical species during estuarine mixing. In: Martin, J.M., Burtor, J.D., Eisma, D. (Eds.), *River Inputs to Ocean Systems*. UNEP/UNESCO, Paris.

Shimmield, G.B., Price, N.B., 1986. The behaviour of molybdenum and manganese during early sediment diagenesis—offshore Baja California, Mexico. *Mar. Chem.* **19**, 261–280.

Shippers, A., Jørgensen, B.B., 2001. Oxidation of pyrite and iron sulfide by manganese dioxide in marine sediments. *Geochim. Cosmochim. Acta* **65**, 915–922.

Slaveck, J., Wold, J., Pickering, W.F., 1982. Extraction of metal ions associated with humic acids. *Talanta* **29**, 743–750.

Sottolichio, A., Castaing, P., 1999. A synthesis on seasonal dynamics of highly-concentrated structures in the Gironde estuary. *C.R. Acad. Sci. Paris, Earth Planet. Sci.* **329**, 795–800.

Stookey, L.L., 1970. Ferrozine–A new spectrophotometric reagent for iron. *Anal. Chem.* **42**, 779–781.

Stumm, W., Morgan, J.J., 1996. *Aquatic Geochemistry*, third ed. John Wiley & Sons.

Suits, N.S., Arthur, M.A., 2000. Bacterial production of anomalously high dissolved sulfate concentrations in Peru slope sediments: steady-state sulfur oxidation, or transient response to end of El Niño. *Deep-Sea Res. I* **47**, 1829–1853.

Tack, F.M.G., Vossius, H.A.H., Verloo, M.G., 1996. A comparison between sediment metal fractions, obtained from sequential extraction and estimated from single samples. *Intern. J. Environ. Anal. Chem.* **63**, 61–66.

Tang, D., Warnken, K.W., Santschi, P.H., 2002. Distribution and partitioning of trace metals (Cd, Cu, Ni, Pb, Zn) in Galveston Bay waters. *Mar. Chem.* **78**, 29–45.

Tebo, B.M., Obraztsova, A.Y., 1998. Sulfate-reducing bacterium grows with Cr(VI), U(VI), Mn(IV), and Fe(III) as electron acceptors. *FEMS Microbiol. Lett.* **162**, 193–198.

Tessier, A., Campbell, P.G.C., Bisson, M., 1979. Sequential extraction procedure for the speciation of particulate trace metals. *Anal. Chem.* **51**, 844–851.

Tipping, E., Hurley, M.A., 1992. A unifying model of cation binding by humic substances. *Geochim. Cosmochim. Acta* **56**, 3627–3641.

Trefy, J.H., Metz, S., 1989. Role of hydrothermal precipitates in geochemical cycling of vanadium. *Nature* **342**, 531–533.

Tseng, C.M., Amouroux, D., Abril, G., Tessier, E., Etcheber, H., Donard, O.F.X., 2001. Speciation of mercury in a fluid mud profile of a highly turbid macrotidal estuary (Gironde, France). *Environ. Sci. Technol.* **35**, 2627–2633.

Turner, A., Millward, G.E., 1993. Partitioning of trace metals in a macrotidal estuary. Implications for contaminant transport models. *Estuar. Coast. Shelf Sci.* **39**, 45–58.

Viollier, E., Inglett, P.W., Hunter, K., Roychoudhury, A.N., Van Capellen, P., 2000. The ferrozine method revisited: Fe(II)/Fe(III) determination in natural waters. *Appl. Geochem.* **15**, 785–790.

Wersin, P., Hochella Jr., M.F., Persson, P., Redden, G., Leckie, J.O., Harris, D.W., 1994. Interaction between aqueous uranium (VI) and sulfide minerals: spectroscopic evidence for sorption and reduction. *Geochim. Cosmochim. Acta* **58**, 2829–2843.

Whiteley, J.D., Pearce, N.J.G., 2003. Metal distribution during diagenesis in the contaminated sediments of Dulas Bay, Anglesey, N. Wales, UK. *Appl. Geochem.* **18**, 901–913.

Wielinga, B., Bostick, B., Hansel, C.M., Rosenzweig, R.F., Fendorf, S., 2000. Inhibition of bacterially promoted uranium reduction: ferric (hydr)oxides as a competitive electron acceptors. *Environ. Sci. Technol.* **34**, 2190–2195.

Widerlund, A., Ingri, J., 1995. Early diagenesis of arsenic in sediments of the Kalix River estuary, northern Sweden. *Chem. Geol.* **125**, 185–196.

Widerlund, A., 1996. Early diagenetic remobilization of copper in near-shore marine sediments: a quantitative pore-water model. *Mar. Chem.* **54**, 41–53.

Yao, W., Millero, F.J., 1996. Oxidation of hydrogen sulfide by hydrous Fe(III) oxides in seawater. *Mar. Chem.* **52**, 1–16.

Zheng, Y., Anderson, R., van Geen, A., Kawabara, J., 2000. Authigenic molybdenum formation in marine sediments: A link to pore water sulfide in the Santa Barbara Basin. *Geochim. Cosmochim. Acta* **64**, 4165–4178.

Zheng, Y., Anderson, R., van Geen, A., Fleisher, M.Q., 2002. Remobilization of authigenic uranium in marine sediments by bioturbation. *Geochim. Cosmochim. Acta* **66**, 1759–1772.

Zhorov, V.A., Boguslavskiy, S.G., Babinets, A., Solov'Yeva, L.V., Kirchanova, A.I., Kir'yakov, P.A., 1982. Geochemistry of uranium in the Black Sea. *Geochim. Cosmochim. Acta* **19**, 191–200.

Zwolsman, J.J.G., Van Eck, B.T.M., Van Der Weijden, C.H., 1997. Geochemistry of dissolved trace metals (cadmium, copper, zinc) in the Scheldt estuary, southwestern Netherlands: impact of seasonal variability. *Geochim. Cosmochim. Acta* **61**, 1635–1652.

Zwolsman, J.J.G., Van Eck, G.T.M., 1999. Geochemistry of major elements and trace metals in suspended matter of the Scheldt estuary, southwest Netherlands. *Mar. Chem.* **66**, 91–111.